



#### Available online at www.sciencedirect.com

## **ScienceDirect**

Computer methods in applied mechanics and engineering

Comput. Methods Appl. Mech. Engrg. 345 (2019) 1007–1032

www.elsevier.com/locate/cma

# A posteriori error estimates for the Stokes problem with singular sources

Alejandro Allendes<sup>a</sup>, Enrique Otárola<sup>a,\*</sup>, Abner J. Salgado<sup>b</sup>

<sup>a</sup> Departamento de Matemática, Universidad Técnica Federico Santa María, Valparaíso, Chile
<sup>b</sup> Department of Mathematics, University of Tennessee, Knoxville, TN 37996, USA

Received 26 June 2018; received in revised form 19 October 2018; accepted 8 November 2018 Available online 27 November 2018

#### **Abstract**

We propose a posteriori error estimators for classical low-order inf–sup stable and stabilized finite element approximations of the Stokes problem with singular sources in two and three dimensional Lipschitz, but not necessarily convex, polytopal domains. The designed error estimators are proven to be reliable and locally efficient. On the basis of these estimators we design a simple adaptive strategy that yields optimal rates of convergence for the numerical examples that we perform.

© 2018 Elsevier B.V. All rights reserved.

MSC: 35Q35; 35Q30; 35R06; 76Dxx; 65N15; 65N30; 65N50

Keywords: A posteriori error estimates; Stokes equations; Dirac measures; Muckenhoupt weights

#### 1. Introduction

The purpose of this work is the design and analysis of a posteriori error estimates for low-order inf–sup stable and stabilized finite element approximations of the Stokes problem

$$\begin{cases}
-\Delta \mathbf{u} + \nabla p = \mathbf{F} \delta_z, & \text{in } \Omega, \\
\text{div } \mathbf{u} = 0, & \text{in } \Omega, \\
\mathbf{u} = 0, & \text{on } \partial \Omega,
\end{cases}$$
(1)

where, for  $d \in \{2, 3\}$ ,  $\Omega$  denotes a bounded polytope of  $\mathbb{R}^d$  with Lipschitz boundary,  $\delta_z$  corresponds to the Dirac delta supported at the interior point  $z \in \Omega$  and  $\mathbf{F} \in \mathbb{R}^d$ .

As it is well known, system (1) is one of the simplest systems of equations that describes the motion of an incompressible fluid. Here **u** represents the velocity of the fluid, p the pressure, and  $\mathbf{F}\delta_z$  is an externally applied

E-mail addresses: alejandro.allendes@usm.cl (A. Allendes), enrique.otarola@usm.cl (E. Otárola), asalgad1@utk.edu (A.J. Salgado). URLs: http://aallendes.mat.utfsm.cl/ (A. Allendes), http://eotarola.mat.utfsm.cl/ (E. Otárola), http://www.math.utk.edu/~abnersg (A.J. Salgado).

AA has been partially supported by CONICYT (Chile) through FONDECYT project 1170579. EO has been partially supported by CONICYT (Chile) through FONDECYT project 11180193. AJS has been partially supported by NSF (USA) grant DMS-1720213.

<sup>\*</sup> Corresponding author.

force. Notice that, for simplicity, we have taken the viscosity to be equal to one. The first equation represents the conservation of momentum and the second one (incompressibility) the conservation of mass.

While it is fair to say that the study of approximation techniques for (1) and related models in a standard setting is matured and well understood [1,2], recent applications and models have emerged where the motion of a fluid is described by (1) or a small variation of it, but due to the material properties (encoded by the viscosity) or, as is our interest here, the singularity of forces  $\mathbf{F}\delta_z$ , the problem must be understood in a completely different setting and rigorous approximation techniques are nonexistent. For instance, [3] models the motion of active thin structures by using a generalization of (1), where the right hand side is a linear combination of the terms we have there. The author of this work proposes a numerical scheme but its stability and convergence properties are not investigated. Another instance where a singular force like that of (1) may occur, see [4] and [5,6], is in a PDE constrained optimization problem where the state is governed by a standard Stokes problem, but the objective contains a point value of  $\mathbf{u}$ . The idea in this problem is that one tries to optimize the flow profile so as to match the velocity at a certain point. If one were to write the optimality conditions for this problem the so-called adjoint variable will be governed by a slight modification of (1) where z is the observation point. Finally, [7] studies a class of asymptotically Newtonian fluids (Newtonian under large shear rates) under singular forcing. The authors show existence and uniqueness as well as some regularity results. In this respect, our work can be understood as an initial step towards the a posteriori error estimation of such fluids.

The examples presented above justify the need to develop robust solution techniques for the numerical approximation of solutions to (1), and this is the purpose of this work. The key observation that will allow us to handle the singularity in this problem is that there is a Muckenhoupt weight  $\omega$ , related to the distance to z, such that  $\delta_z \in H^{-1}(\omega, \Omega)$ . In light of this, we propose to study numerical methods in Muckenhoupt weighted Sobolev spaces, in particular, we shall be concerned with the design and analysis of a posteriori error estimates for problem (1) on such spaces. The analysis relies on the following ingredients that are available in the literature: Muckenhoupt weights and weighted norm inequalities [8–11], stability and approximation properties of the quasi-interpolation operator of [10,12] on weighted Sobolev spaces, and stability properties for bubble functions in weighted norms [13]. These ingredients allow us to conclude that the error estimators defined below in (37) and (71), for inf–sup stable and stabilized finite element approximations, respectively, are reliable and locally efficient.

We finally comment that, since  $\delta_z$  is very singular, it is not expected for the pair ( $\mathbf{u}$ , p) to have any regularity properties beyond those merely needed for the problem to be well-posed. For this reason a priori error estimates in their natural norms might not carry much value in this setting: a quasi-best approximation result  $\grave{a}$  la Céa could be derived, but rates of convergence will not follow from this. On the other hand, using duality techniques, it might be possible to obtain error estimates in lower order norms. In either of these two cases, the analysis will rely, in particular, on a discrete inf–sup condition for the bilinear form of the Dirichlet Laplace operator over a discrete space of functions with vanishing divergence. This is nontrival and will be deferred to a future study.

### 1.1. Structure of the paper

Our presentation is organized as follows. We set notation in Section 2, where we also recall basic facts about weights and introduce the weighted spaces we shall work with. In Section 3, we introduce a saddle point formulation of the Stokes problem (1) and review well-posedness results. Section 4 is one of the highlights of our work. There we propose an a posteriori error estimator for inf—sup stable finite element approximations of the Stokes problem (1); the devised error estimator is proven to be locally efficient and globally reliable. In Section 5 we extend the results obtained in Section 4 to the case when stabilized finite element approximations are considered. We conclude, in Section 6, with a series of numerical experiments that illustrate our theory.

## 2. Notation and preliminaries

Let us fix the notation and conventions in which we will operate. Throughout this work  $d \in \{2, 3\}$  and  $\Omega \subset \mathbb{R}^d$  is an open and bounded polytopal domain with Lipschitz boundary  $\partial \Omega$ . Notice that we do not assume that  $\Omega$  is convex. If  $\mathcal{W}$  and  $\mathcal{Z}$  are Banach function spaces, we write  $\mathcal{W} \hookrightarrow \mathcal{Z}$  to denote that  $\mathcal{W}$  is continuously embedded in  $\mathcal{Z}$ . We denote by  $\mathcal{W}'$  and  $\|\cdot\|_{\mathcal{W}}$  the dual and the norm of  $\mathcal{W}$ , respectively.

For  $E \subset \bar{\Omega}$  of finite Hausdorff *i*-dimension,  $i \in \{1, ..., d\}$ , we denote its measure by |E|. If E is such a set and  $f : E \to \mathbb{R}$  we denote its mean value by

$$\oint_E f = \frac{1}{|E|} \int_E f.$$

The relation  $a \lesssim b$  indicates that  $a \leq Cb$ , with a constant C that depends neither on a, b nor the discretization parameters. The value of C might change at each occurrence.

## 2.1. Weights and weighted spaces

By a weight, we shall mean a locally integrable function  $\omega$  on  $\mathbb{R}^d$  such that  $\omega(x) > 0$  a.e.  $x \in \mathbb{R}^d$ . A particular class of weights, that will be of importance in our work, is the so-called Muckenhoupt class  $A_2$  [14]: If  $\omega$  is a weight, we say that  $\omega \in A_2$  if

$$[\omega]_{A_2} := \sup_{B} \left( \int_{B} \omega \right) \left( \int_{B} \omega^{-1} \right) < \infty, \tag{2}$$

where the supremum is taken over all balls B in  $\mathbb{R}^d$ . In what follows, for  $\omega \in A_2$ , we call  $[\omega]_{A_2}$  the *Muckenhoupt characteristic* of  $\omega$ .

We refer the reader to [8–11] for the basic facts about Muckenhoupt classes and the ensuing weighted spaces. Here we only mention an example of an  $A_2$  weight which will be essential in the analysis presented below. Let  $z \in \Omega$  be an interior point of  $\Omega$  and, for  $\alpha \in \mathbb{R}$ , define

$$\mathbf{d}_{z}^{\alpha}(x) = |x - z|^{\alpha}.\tag{3}$$

We then have that  $d_{\tau}^{\alpha} \in A_2$  provided that  $\alpha \in (-d, d)$ .

It is also important to notice that, in the previous example, since  $z \in \Omega$  there is a neighborhood of  $\partial \Omega$  where the weight  $d_z^{\alpha}$  has no degeneracies or singularities. In fact, it is continuous and strictly positive. Consequently, we have that the weight  $d_z^{\alpha}$  belongs to the class  $A_2(\Omega)$ , introduced in [15, Definition 2.5], and which we define as follows.

**Definition 1** (*Class*  $A_2(\Omega)$ ). Let  $\Omega \subset \mathbb{R}^d$  be a Lipschitz domain. We say that  $\omega \in A_2$  belongs to  $A_2(\Omega)$  if there is an open set  $\mathcal{G} \subset \Omega$ , and positive constants  $\varepsilon > 0$  and  $\omega_l > 0$  such that:

- 1.  $\{x \in \Omega : \operatorname{dist}(x, \partial \Omega) < \varepsilon\} \subset \mathcal{G}$ ,
- 2.  $\omega|_{\bar{\mathcal{G}}} \in C(\bar{\mathcal{G}})$ , and
- 3.  $\omega_l \leq \omega(x)$  for all  $x \in \bar{\mathcal{G}}$ .

The fact that  $d_z^{\alpha}$  belongs to the restricted class  $A_2(\Omega)$  has been shown to be crucial in the analysis of [16] that guarantees the well-posedness of problem (1) in weighted Sobolev spaces. We will recall these facts in Section 3.

For  $\alpha \in (-d, d)$  and an open set  $E \subset \Omega$ , we define

$$L^{2}(\mathsf{d}_{z}^{\pm\alpha},E) := \left\{ v \in L^{1}_{\mathrm{loc}}(E) : \|v\|_{L^{2}(\mathsf{d}_{z}^{\pm\alpha},E)} := \left( \int_{E} \mathsf{d}_{z}^{\pm\alpha} |v|^{2} \right)^{\frac{1}{2}} < \infty \right\}$$

and

$$H^1(\mathsf{d}_z^{\pm lpha},E) \coloneqq \{v \in L^2(\mathsf{d}_z^{\pm lpha},E) : |\nabla v| \in L^2(\mathsf{d}_z^{\pm lpha},E)\}$$

with norm

$$\|v\|_{H^{1}(\mathsf{d}_{z}^{\pm\alpha},E)} := \left(\|v\|_{L^{2}(\mathsf{d}_{z}^{\pm\alpha},E)}^{2} + \|\nabla v\|_{L^{2}(\mathsf{d}_{z}^{\pm\alpha},E)}^{2}\right)^{\frac{1}{2}}.$$
(4)

We also define  $H_0^1(\mathsf{d}_z^{\pm\alpha}, E)$  as the closure of  $C_0^\infty(E)$  in  $H^1(\mathsf{d}_z^{\pm\alpha}, E)$ . In view of the fact that, for  $\alpha \in (-d, d)$ , the weight  $\mathsf{d}_z^{\pm\alpha}$  belongs to  $A_2$ , we conclude that the spaces  $L^2(\mathsf{d}_z^{\pm\alpha}, E)$  and  $H^1(\mathsf{d}_z^{\pm\alpha}, E)$  are Hilbert [11, Proposition 2.1.2] and that smooth functions are dense [11, Corollary 2.1.6]; see also [9, Theorem 1]. In addition, [17, Theorem 1.3] guarantees the existence of a weighted Poincaré inequality which, in turn, implies that over  $H_0^1(\mathsf{d}_z^{\pm\alpha}, \Omega)$  the seminorm

 $\|\nabla v\|_{L^2(\mathbf{d}_{\varepsilon}^{\pm \alpha},\Omega)}$  is an equivalent norm to the one defined in (4) for  $E=\Omega$ . We also introduce the weighted space of vector-valued functions and the norm

$$\mathbf{H}_{0}^{1}(\mathsf{d}_{z}^{\pm\alpha},E) = [H_{0}^{1}(\mathsf{d}_{z}^{\pm\alpha},E)]^{d}, \quad \|\nabla\mathbf{v}\|_{\mathbf{L}^{2}(\mathsf{d}_{z}^{\pm\alpha},E)} \coloneqq \left(\sum_{i=1}^{d} \|\nabla v_{i}\|_{L^{2}(\mathsf{d}_{z}^{\pm\alpha},E)}^{2}\right)^{\frac{1}{2}},$$

where  $\mathbf{v} = (v_1, \dots, v_d)^{\mathsf{T}}$ .

For  $\alpha \in (-d, d)$  we also introduce the product spaces

$$\mathcal{X}(E) = \mathbf{H}_0^1(\mathbf{d}_z^{\alpha}, E) \times L^2(\mathbf{d}_z^{\alpha}, E) / \mathbb{R}, \quad \mathcal{Y}(E) = \mathbf{H}_0^1(\mathbf{d}_z^{-\alpha}, E) \times L^2(\mathbf{d}_z^{-\alpha}, E) / \mathbb{R}, \tag{5}$$

which we endow with the norms

$$\|(\mathbf{w}, r)\|_{\mathcal{X}(E)} = \left(\|\nabla \mathbf{w}\|_{\mathbf{L}^{2}(\mathsf{d}_{z}^{\alpha}, E)}^{2} + \|r\|_{L^{2}(\mathsf{d}_{z}^{\alpha}, E)/\mathbb{R}}^{2}\right)^{\frac{1}{2}}$$
(6)

and

$$\|(\mathbf{v},q)\|_{\mathcal{Y}(E)} = \left(\|\nabla \mathbf{v}\|_{\mathbf{L}^{2}(\mathbf{d}_{z}^{-\alpha},E)}^{2} + \|q\|_{L^{2}(\mathbf{d}_{z}^{-\alpha},E)/\mathbb{R}}^{2}\right)^{\frac{1}{2}},\tag{7}$$

respectively. When  $E = \Omega$ , and in order to simplify the presentation of the material, we write  $\mathcal{X} = \mathcal{X}(\Omega)$  and  $\mathcal{Y} = \mathcal{Y}(\Omega)$ .

The following continuous embedding results will be instrumental in the analysis that follows.

**Proposition 2** (Continuous Embeddings I). Let E be an open subset of  $\Omega \subset \mathbb{R}^d$  and  $\alpha \in (-d, d)$ . Then, we have the following continuous embeddings

$$\mathbf{L}^2(\mathsf{d}_z^{-\alpha}, E) \hookrightarrow \mathbf{L}^1_{\mathrm{loc}}(E), \qquad \mathbf{L}^2(\mathsf{d}_z^{\alpha}, E) \hookrightarrow \mathbf{L}^1_{\mathrm{loc}}(E).$$
 (8)

**Proof.** Let  $\mathbf{v} \in \mathbf{L}^2(\mathsf{d}_z^\alpha, E)$  and  $B \subset E$  be a ball. A trivial application of the Cauchy–Schwarz inequality reveals that

$$\int_{B} |\mathbf{v}| = \int_{B} \mathsf{d}_{z}^{\frac{\alpha}{2}} |\mathbf{v}| \mathsf{d}_{z}^{-\frac{\alpha}{2}} \leq \left( \int_{B} \mathsf{d}_{z}^{\alpha} |\mathbf{v}|^{2} \right)^{\frac{1}{2}} \left( \int_{B} \mathsf{d}_{z}^{-\alpha} \right)^{\frac{1}{2}} \lesssim \left( \int_{B} \mathsf{d}_{z}^{\alpha} |\mathbf{v}|^{2} \right)^{\frac{1}{2}},$$

where, to obtain the last inequality, we have used that, since  $\alpha \in (-d,d)$ ,  $\mathsf{d}_z^{-\alpha}$  is a weight, i.e., a nonnegative and locally integrable function. This yields the continuous embedding  $\mathbf{L}^2(\mathsf{d}_z^\alpha,E) \hookrightarrow \mathbf{L}^1_{\mathrm{loc}}(E)$ . The proof of the continuous embedding  $\mathbf{L}^2(\mathsf{d}_z^{-\alpha},E) \hookrightarrow \mathbf{L}^1_{\mathrm{loc}}(E)$  is similar.  $\square$ 

**Proposition 3** (Continuous Embeddings II). Let E be an open subset of  $\Omega \subset \mathbb{R}^d$ . If  $\alpha \in (0, d)$ , then we have the following continuous embeddings

$$\mathbf{H}_0^1(\mathbf{d}_z^{-\alpha}, E) \hookrightarrow \mathbf{H}_0^1(E) \hookrightarrow \mathbf{H}_0^1(\mathbf{d}_z^{\alpha}, E). \tag{9}$$

**Proof.** The proof follows from the fact that, since  $\alpha \in (0, d)$ , then  $\max_{x \in E} \mathsf{d}_z^{\alpha}(x)$  is uniformly bounded. In fact, for  $\mathbf{v} \in \mathbf{C}_0^{\infty}(E)$ , we have that

$$\int_{E} |\nabla \mathbf{v}|^{2} \leq \max_{x \in E} \mathsf{d}_{z}^{\alpha}(x) \int_{E} \mathsf{d}_{z}^{-\alpha} |\nabla \mathbf{v}|^{2}, \qquad \int_{E} \mathsf{d}_{z}^{\alpha} |\nabla \mathbf{v}|^{2} \leq \max_{x \in E} \mathsf{d}_{z}^{\alpha}(x) \int_{E} |\nabla \mathbf{v}|^{2}.$$

The embeddings described in (9) now follow from a density argument. This concludes the proof.  $\Box$ 

## 3. The Stokes problem with Dirac sources

Having set up the needed functional setting, we now begin with the systematic study of problem (1). First, we provide a motivation for the use of weights.

### 3.1. Motivation

Let us assume that (1) is posed over the whole space  $\mathbb{R}^d$ . If that is the case, the results of [18, Section IV.2] provide the following asymptotic behavior of the solution ( $\mathbf{u}$ , p) to problem (1) near the point z:

$$|\nabla \mathbf{u}(x)| \approx |x - z|^{1 - d} \quad \text{and} \quad |p(x)| \approx |x - z|^{1 - d}. \tag{10}$$

On the basis of these asymptotic estimates, basic computations reveal that

$$\alpha \in (d-2,\infty) \implies \int_{\Omega} \mathsf{d}_{z}^{\alpha} |\nabla \mathbf{u}|^{2} < \infty, \quad \int_{\Omega} \mathsf{d}_{z}^{\alpha} |p|^{2} < \infty.$$

This heuristic suggests to seek solutions to problem (1) in weighted Sobolev spaces [7,16]. In what follows we will make these considerations rigorous.

## 3.2. Saddle point formulation

The motivation of the previous paragraph suggests that we seek for solutions of (1) in the weighted spaces defined in Section 2. To accomplish this task, we define the bilinear forms

$$a: \mathbf{H}_{0}^{1}(\mathsf{d}_{z}^{\alpha}, \Omega) \times \mathbf{H}_{0}^{1}(\mathsf{d}_{z}^{-\alpha}, \Omega) \to \mathbb{R},$$

$$a(\mathbf{w}, \mathbf{v}) := \int_{\Omega} \nabla \mathbf{w} : \nabla \mathbf{v} = \sum_{i=1}^{d} \int_{\Omega} \nabla \mathbf{w}_{i} \cdot \nabla \mathbf{v}_{i}$$
(11)

and

$$b: \mathbf{H}_0^1(\mathbf{d}_z^{\pm \alpha}, \Omega) \times L^2(\mathbf{d}_z^{\mp \alpha}, \Omega) \to \mathbb{R},$$

$$b(\mathbf{v}, q) := -\int_{\Omega} q \operatorname{div} \mathbf{v}.$$
(12)

The weak formulation of problem (1) that we shall consider is: Find  $(\mathbf{u}, p) \in \mathbf{H}_0^1(\mathbf{d}_z^{\alpha}, \Omega) \times L^2(\mathbf{d}_z^{\alpha}, \Omega)/\mathbb{R}$  such that

$$\begin{cases}
a(\mathbf{u}, \mathbf{v}) + b(\mathbf{v}, p) = \langle \mathbf{F} \delta_z, \mathbf{v} \rangle, & \forall \mathbf{v} \in \mathbf{H}_0^1(\mathbf{d}_z^{-\alpha}, \Omega), \\
b(\mathbf{u}, q) = 0, & \forall q \in L^2(\mathbf{d}_z^{-\alpha}, \Omega) / \mathbb{R},
\end{cases}$$
(13)

where  $\langle \cdot, \cdot \rangle$  denotes the duality pairing between  $\mathbf{H}_0^1(\mathsf{d}_z^{-\alpha}, \Omega)'$  and  $\mathbf{H}_0^1(\mathsf{d}_z^{-\alpha}, \Omega)$ . We must immediately comment that, in order to guarantee that  $\delta_z \in H_0^1(\mathsf{d}_z^{-\alpha}, \Omega)'$ , and thus that  $\langle \mathbf{F}\delta_z, \mathbf{v} \rangle$  is well-defined for  $\mathbf{v} \in \mathbf{H}_0^1(\mathsf{d}_z^{-\alpha}, \Omega)$ , the parameter  $\alpha$  should be restricted to belong to the interval (d-2, d) [19, Lemma 7.1.3].

We now present a trivial reformulation of problem (1). To accomplish this task, we define the bilinear form  $c: \mathcal{X} \times \mathcal{Y} \to \mathbb{R}$  by

$$c((\mathbf{w}, r), (\mathbf{v}, q)) := a(\mathbf{w}, \mathbf{v}) + b(\mathbf{v}, r) - b(\mathbf{w}, q)$$

$$\tag{14}$$

with norm

$$||c|| = \sup_{(\mathbf{0},0) \neq (\mathbf{w},r) \in \mathcal{X}} \sup_{(\mathbf{0},0) \neq (\mathbf{v},q) \in \mathcal{Y}} \frac{c((\mathbf{w},r),(\mathbf{v},q))}{||(\mathbf{w},r)||_{\mathcal{X}} ||(\mathbf{v},q)||_{\mathcal{Y}}},$$
(15)

where the product spaces  $\mathcal{X}$  and  $\mathcal{Y}$  were defined in (5).

The aforementioned reformulation of problem (1) thus reads as follows: Find  $(\mathbf{u}, p) \in \mathcal{X}$  such that

$$c((\mathbf{u}, p), (\mathbf{v}, q)) = \langle \mathbf{F} \delta_z, \mathbf{v} \rangle \quad \forall (\mathbf{v}, q) \in \mathcal{Y}.$$
 (16)

It has been recently proved in [16] that, since  $d_z^{\alpha} \in A_2(\Omega)$ , problem (16) admits a unique solution ( $\mathbf{u}, p$ )  $\in \mathcal{X} = \mathbf{H}_0^1(d_z^{\alpha}, \Omega) \times L^2(d_z^{\alpha}, \Omega)/\mathbb{R}$  for  $\alpha \in (d-2, d)$ . In addition, the following a priori error estimate was also derived in [16, Theorem 14]:

$$\|\nabla \mathbf{u}\|_{\mathbf{L}^{2}(\mathsf{d}_{z}^{\alpha},\Omega)} + \|p\|_{L^{2}(\mathsf{d}_{z}^{\alpha},\Omega)/\mathbb{R}} \lesssim |\mathbf{F}| \|\delta_{z}\|_{\mathbf{H}_{0}^{1}(\mathsf{d}_{z}^{\alpha},\Omega)'}. \tag{17}$$

With such a well-posedness result at hand, we can thus invoke a result by Nečas, see [20, Théorème 6.3.1], [21, Théorèmes 3.1 et 3.2], and [22, Theorem 2.2 and Corollary 2.1], to conclude the existence of a constant  $\beta > 0$  such that

$$\inf_{\substack{(\mathbf{0},0)\neq(\mathbf{w},r)\in\mathcal{X}\\(\mathbf{0},0)\neq(\mathbf{v},q)\in\mathcal{Y}\\(\mathbf{0},0)\neq(\mathbf{v},q)\in\mathcal{Y}}} \frac{c((\mathbf{w},r),(\mathbf{v},q))}{\|(\mathbf{w},r)\|_{\mathcal{X}}\|(\mathbf{v},q)\|_{\mathcal{Y}}} = 
\inf_{\substack{(\mathbf{0},0)\neq(\mathbf{v},q)\in\mathcal{Y}\\(\mathbf{0},0)\neq(\mathbf{w},r)\in\mathcal{X}}} \frac{c((\mathbf{w},r),(\mathbf{v},q))}{\|(\mathbf{w},r)\|_{\mathcal{X}}\|(\mathbf{v},q)\|_{\mathcal{Y}}} = \beta.$$
(18)

## 4. Inf-sup stable finite element spaces

Having shown the well-posedness of (13), we can now begin with its numerical approximation and the analysis of the ensuing methods. We first introduce some terminology and a few basic ingredients that will be common to all our methods.

## 4.1. Triangulation

We consider  $\mathscr{T} = \{T\}$  to be a conforming partition of  $\bar{\Omega}$  into closed simplices T with size  $h_T = \operatorname{diam}(T)$  and define  $h_{\mathscr{T}} = \max_{T \in \mathscr{T}} h_T$ . We denote by  $\mathbb{T}$  the collection of conforming and shape regular meshes that are refinements of an initial mesh  $\mathscr{T}_0$  [1,23].

We denote by  $\mathscr{S}$  the set of internal (d-1)-dimensional interelement boundaries S of  $\mathscr{T}$ . For  $S \in \mathscr{S}$ , we indicate by  $h_S$  the diameter of S. If  $T \in \mathscr{T}$ , we define  $\mathscr{S}_T$  as the subset of  $\mathscr{S}$  that contains the sides of T. For  $S \in \mathscr{S}$ , we set  $\mathcal{N}_S = \{T^+, T^-\}$ , where  $T^+, T^- \in \mathscr{T}$  are such that  $S = T^+ \cap T^-$ , in other words,  $\mathcal{N}_S$  denotes the subset of  $\mathscr{T}$  that contains the two elements of  $\mathscr{T}$  that have S as a side. For  $T \in \mathscr{T}$ , we define the following *stars* or *patches* associated with the element T

$$\mathcal{N}_T := \left\{ T' \in \mathcal{T} : \mathcal{S}_T \cap \mathcal{S}_{T'} \neq \emptyset \right\}. \tag{19}$$

and

$$S_T := \bigcup_{T' \in \mathscr{T}: T \cap T' \neq \emptyset} T'. \tag{20}$$

Having defined our mesh we introduce two classes of finite element approximations, the ensuing finite element schemes, and provide an analysis for them.

### 4.2. Stable finite element approximations

In the literature, several finite element approximations have been proposed and analyzed to approximate the solution to the Stokes problem (13) when the forcing term of the momentum equation is not singular; see, for instance, [1, Section 4], [2, Chapter II], and references therein. If, given a mesh  $\mathscr{T} \in \mathbb{T}$ , we denote by  $\mathbf{V}(\mathscr{T})$  and  $\mathcal{P}(\mathscr{T})$  the finite element spaces that approximate the velocity field and the pressure, respectively, then the following elections are popular:

(a) The *mini* element [24], [1, Section 4.2.4]: in this case,

$$\mathbf{V}(\mathscr{T}) = \left\{ \mathbf{v}_{\mathscr{T}} \in \mathbf{C}(\bar{\Omega}) : \forall T \in \mathscr{T}, \mathbf{v}_{\mathscr{T}}|_{T} \in [\mathbb{P}_{1}(T) \oplus \mathbb{B}(T)]^{d} \right\} \cap \mathbf{H}_{0}^{1}(\Omega), \tag{21}$$

$$\mathcal{P}(\mathcal{T}) = \left\{ q_{\mathcal{T}} \in L^{2}(\Omega) / \mathbb{R} \cap C(\bar{\Omega}) : \forall T \in \mathcal{T}, q_{\mathcal{T}}|_{T} \in \mathbb{P}_{1}(T) \right\}. \tag{22}$$

 $\mathbb{B}(T)$  denotes the space spanned by local bubble functions.

(b) The classical Taylor–Hood element [25,26], [1, Section 4.2.5]: in this scenario,

$$\mathbf{V}(\mathscr{T}) = \left\{ \mathbf{v}_{\mathscr{T}} \in \mathbf{C}(\bar{\Omega}) : \forall T \in \mathscr{T}, \mathbf{v}_{\mathscr{T}}|_{T} \in \mathbb{P}_{2}(T)^{d} \right\} \cap \mathbf{H}_{0}^{1}(\Omega), \tag{23}$$

$$\mathcal{P}(\mathcal{T}) = \left\{ q_{\mathcal{T}} \in L^2(\Omega) / \mathbb{R} \cap C(\bar{\Omega}) : \forall T \in \mathcal{T}, q_{\mathcal{T}}|_T \in \mathbb{P}_1(T) \right\}. \tag{24}$$

The aforementioned pairs of finite element spaces  $(V(\mathcal{T}), \mathcal{P}(\mathcal{T}))$  satisfy the following compatibility condition [1, Proposition 4.13]: there exists a positive constant  $\gamma$  such that, for all  $\mathcal{T} \in \mathbb{T}$ ,

$$\inf_{0 \neq q_{\mathscr{T}} \in \mathcal{P}(\mathscr{T})} \sup_{\mathbf{0} \neq \mathbf{v}_{\mathscr{T}} \in \mathbf{V}(\mathscr{T})} \frac{b(\mathbf{v}_{\mathscr{T}}, q_{\mathscr{T}})}{\|\nabla \mathbf{v}_{\mathscr{T}}\|_{\mathbf{L}^{2}(\Omega)} \|q_{\mathscr{T}}\|_{L^{2}(\Omega)/\mathbb{R}}} \geq \gamma. \tag{25}$$

We refer the reader to [1, Lemma 4.20 and Lemma 4.24] for a proof.

We observe now that, since the  $d_z^{\alpha}$  is a weight, we thus have, for the elections given by (21)–(24), that

$$\mathbf{V}(\mathscr{T}) \subset \mathbf{H}_0^1(\mathsf{d}_{\tau}^{\pm \alpha}, \Omega), \qquad \mathcal{P}(\mathscr{T}) \subset L^2(\mathsf{d}_{\tau}^{\pm \alpha}, \Omega)/\mathbb{R}.$$

Consequently, we can consider the following finite element approximation of problem (13): Find  $(\mathbf{u}_{\mathscr{T}}, p_{\mathscr{T}}) \in \mathbf{V}(\mathscr{T}) \times \mathcal{P}(\mathscr{T})$  such that

$$\begin{cases}
a(\mathbf{u}_{\mathscr{T}}, \mathbf{v}_{\mathscr{T}}) + b(\mathbf{v}_{\mathscr{T}}, p_{\mathscr{T}}) = \mathbf{F} \cdot \mathbf{v}_{\mathscr{T}}(z), & \forall \mathbf{v}_{\mathscr{T}} \in \mathbf{V}(\mathscr{T}), \\
b(\mathbf{u}_{\mathscr{T}}, q_{\mathscr{T}}) = 0, & \forall q_{\mathscr{T}} \in \mathcal{P}(\mathscr{T}).
\end{cases}$$
(26)

Notice that, since  $\mathbf{v}_{\mathscr{T}} \in \mathbf{C}(\bar{\Omega})$ ,  $\langle \mathbf{F} \delta_z, \mathbf{v}_{\mathscr{T}} \rangle = \mathbf{F} \cdot \mathbf{v}_{\mathscr{T}}(z)$ . In addition, since the bilinear form a is coercive on  $\mathbf{H}_0^1(\Omega) \supset \mathbf{V}(\mathscr{T})$  and the pairs  $(\mathbf{V}(\mathscr{T}), \mathcal{P}(\mathscr{T}))$  satisfy (25), the system (26) has a unique solution for each mesh  $\mathscr{T}$ .

The main issue, however, is not existence of discrete solutions, but the fact that the stability estimates that might be obtained are not in norms that are compatible with those of (13). In what follows we will propose a posteriori error estimators in these natural norms and show their reliability and efficiency.

### 4.3. A quasi-interpolation operator

As it is customary in a posteriori error analysis [27], in order to derive reliability properties for a proposed a posteriori error estimator it is useful to have at hand a suitable quasi-interpolation operator with optimal approximation properties. Since the interest is to approximate rough functions, namely those without point values, the classical Lagrange interpolation operator cannot be applied. Instead, we consider the quasi-interpolation operator  $\Pi_{\mathscr{T}}$ :  $\mathbf{L}^1(\Omega) \to \mathbf{V}(\mathscr{T})$  analyzed in [10]. The construction of  $\Pi_{\mathscr{T}}$  is inspired in the ideas developed by Clément [28], Scott and Zhang [29], and Durán and Lombardi [12]: it is built on local averages over stars and thus well-defined for functions in  $\mathbf{L}^1(\Omega)$ ; it also exhibits optimal approximation properties. In what follows, we shall make use of the following estimates of the local interpolation error. To present them, we first define, for  $T \in \mathscr{T}$ ,

$$D_T := \max_{x \in T} |x - z|. \tag{27}$$

**Proposition 4** (Stability and Interpolation Estimates). Let  $\alpha \in (-d, d)$ , and  $T \in \mathcal{T}$ . Then, for every  $\mathbf{v} \in \mathbf{H}_0^1(\mathsf{d}_z^{\pm \alpha}, \mathcal{S}_T)$ , we have the local stability bound

$$\|\nabla \Pi_{\mathscr{T}}\mathbf{v}\|_{\mathbf{L}^{2}(\mathbf{d}^{\pm \alpha}, T)} \lesssim \|\nabla \mathbf{v}\|_{\mathbf{L}^{2}(\mathbf{d}^{\pm \alpha}, S_{T})} \tag{28}$$

and the interpolation error estimate

$$\|\mathbf{v} - \Pi_{\mathscr{T}}\mathbf{v}\|_{\mathbf{L}^{2}(\mathbf{d}_{\tau}^{\pm\alpha}, T)} \lesssim h_{T} \|\nabla\mathbf{v}\|_{\mathbf{L}^{2}(\mathbf{d}_{\tau}^{\pm\alpha}, \mathcal{S}_{T})},\tag{29}$$

In addition, if  $\alpha \in (d-2, d)$ , then we have that

$$\|\mathbf{v} - \Pi_{\mathscr{T}}\mathbf{v}\|_{L^2(T)} \lesssim h_T D_T^{\frac{\alpha}{2}} \|\nabla \mathbf{v}\|_{\mathbf{L}^2(\mathsf{d}_{\tau}^{-\alpha}, \mathcal{S}_T)}. \tag{30}$$

The hidden constants, in the previous inequalities, are independent of  $\mathbf{v}$ , the cell T, and the mesh  $\mathcal{T}$ .

**Proof.** First, notice that, since  $\alpha \in (-d,d)$ , we have that  $\mathsf{d}_z^{\pm \alpha} \in A_2$ , which implies that, in view of Proposition 2,  $\Pi_{\mathscr{T}}$  is well-defined for functions in  $\mathbf{H}_0^1(\mathsf{d}_z^{\pm \alpha},\mathcal{S}_T)$ . In addition, the theory of [10] can be applied, and thus the local stability bound (28) follows from [10, Lemma 5.1] by setting  $\omega = \mathsf{d}_z^{\pm \alpha}$ . The estimate (29) follows directly from [10, Theorems 5.2 and 5.3] after setting  $\omega = \mathsf{d}_z^{\pm \alpha}$ .

It remains then to prove (30). First, since  $\alpha \in (d-2,d) \subset (0,d)$  we have, according to Proposition 3, that  $\mathbf{H}_0^1(\mathbf{d}_z^{-\alpha}, \mathcal{S}_T) \hookrightarrow \mathbf{H}_0^1(\mathcal{S}_T)$ . Thus, an application of [10, Theorem 5.2 and Theorem 5.3] with  $\omega = 1$ , gives

$$\|\mathbf{v} - \Pi_{\mathscr{T}}\mathbf{v}\|_{L^2(T)} \lesssim h_T \|\nabla \mathbf{v}\|_{\mathbf{L}^2(\mathcal{S}_T)} \lesssim h_T D_T^{\frac{\alpha}{2}} \|\nabla \mathbf{v}\|_{\mathbf{L}^2(\mathbf{d}_{\tau}^{-\alpha},\mathcal{S}_T)},$$

where, in the last step, we used that  $\alpha > 0$  and that, for all  $x \in \mathcal{S}_T$ ,  $\mathbf{d}_{\tau}^{\alpha}(x) \leq D_T^{\alpha}$ .

This concludes the proof.  $\Box$ 

**Proposition 5** (*Trace Interpolation Estimate*). Let  $\alpha \in (d-2,d)$ ,  $T \in \mathcal{T}$ ,  $S \subset \mathcal{S}_T$ , and  $\mathbf{v} \in \mathbf{H}_0^1(\mathsf{d}_z^{-\alpha},\mathcal{S}_T)$ . Then we have the following interpolation error estimate for the trace

$$\|\mathbf{v} - \Pi_{\mathscr{T}}\mathbf{v}\|_{L^2(S)} \lesssim h_T^{\frac{1}{2}} D_T^{\frac{\alpha}{2}} \|\nabla \mathbf{v}\|_{\mathbf{L}^2(\mathsf{d}_{\tau}^{-\alpha}, \mathcal{S}_T)},\tag{31}$$

where the hidden constant is independent of  $\mathbf{v}$ , T, and the mesh  $\mathcal{T}$ .

**Proof.** As a first step, we recall the scaled trace inequality of [22, Corollary 6.1]:

$$\|v\|_{L^2(S)} \lesssim h_S^{-\frac{1}{2}} \|v\|_{L^2(T)} + h_S^{\frac{1}{2}} \|\nabla v\|_{L^2(T)} \quad \forall v \in H^1(T),$$

where  $S \in \mathscr{S}_T$ . In view of the continuous embedding  $\mathbf{H}_0^1(\mathbf{d}_z^{-\alpha}, \mathcal{S}_T) \hookrightarrow \mathbf{H}_0^1(\mathcal{S}_T)$  that was shown in Proposition 3, we can apply the previous bound to the function  $\mathbf{v} - \mathcal{I}_{\mathscr{T}}\mathbf{v} \in \mathbf{H}^1(\mathbf{d}_z^{-\alpha}, \mathcal{S}_T)$ . This, combined with the interpolation error estimate (30), reveals that

$$\|\mathbf{v} - \Pi_{\mathscr{T}}\mathbf{v}\|_{L^{2}(S)} \lesssim h_{S}^{-\frac{1}{2}} h_{T} D_{T}^{\frac{\alpha}{2}} \|\nabla \mathbf{v}\|_{\mathbf{L}^{2}(\mathbf{d}_{\sigma}^{-\alpha}, S_{T})} + h_{S}^{\frac{1}{2}} \|\nabla (\mathbf{v} - \Pi_{\mathscr{T}}\mathbf{v})\|_{\mathbf{L}^{2}(T)}.$$
(32)

To control the second term on the right-hand side of the previous expression, we invoke the stability of the quasiinterpolation operator  $\Pi_{\mathcal{T}}$  in  $H^1$  [10, Lemma 5.1] and, once again, the fact that  $\alpha > 0$  to obtain that

$$\|\nabla(\mathbf{v} - \Pi_{\mathscr{T}}\mathbf{v})\|_{\mathbf{L}^{2}(T)} \lesssim \|\nabla\mathbf{v}\|_{\mathbf{L}^{2}(\mathcal{S}_{T})} \lesssim D_{T}^{\frac{\alpha}{2}} \|\nabla\mathbf{v}\|_{\mathbf{L}^{2}(\mathsf{d}^{-\alpha},\mathcal{S}_{T})}.$$
(33)

Replacing the previous estimate into (32) combined with the fact that  $h_T \approx |T|/|S| \approx h_S$  yields (31) and concludes the proof.  $\Box$ 

With the operator  $\Pi_{\mathcal{T}}$  at hand, and following [27, Section 4.10], we define the following restriction operator

$$Q_{\mathscr{T}}: \mathcal{Y} \longrightarrow \mathbf{V}(\mathscr{T}) \times \mathcal{P}(\mathscr{T}), \qquad (\mathbf{v}, q) \longmapsto (\Pi_{\mathscr{T}}\mathbf{v}, 0), \tag{34}$$

where  $\Pi_{\mathscr{T}}\mathbf{v} = (\Pi_{\mathscr{T}}v_1, \dots, \Pi_{\mathscr{T}}v_d)^{\mathsf{T}}$ .

## 4.4. A posteriori error estimators

We are now ready to introduce an a posteriori error estimator for the finite element approximation (26), on the basis of the discrete pairs  $(V(\mathcal{T}), \mathcal{P}(\mathcal{T}))$  given as in (21)–(22) or (23)–(24), of the Stokes problem (13). To accomplish this task, we first recall the definition of the local distance  $D_T$  given as in (27). We thus define, for  $\alpha \in (d-2, d)$  and  $T \in \mathcal{T}$ , the *element error indicators* 

$$\mathcal{E}_{\alpha}(\mathbf{u}_{\mathscr{T}}, p_{\mathscr{T}}; T) := \left( h_{T}^{2} D_{T}^{\alpha} \| \Delta \mathbf{u}_{\mathscr{T}} - \nabla p_{\mathscr{T}} \|_{\mathbf{L}^{2}(T)}^{2} + \| \operatorname{div} \mathbf{u}_{\mathscr{T}} \|_{L^{2}(\mathsf{d}_{z}^{\alpha}, T)}^{2} + h_{T} D_{T}^{\alpha} \| \| \| (\nabla \mathbf{u}_{\mathscr{T}} - p_{\mathscr{T}} \mathbf{I}) \cdot \mathbf{v} \|_{\mathbf{L}^{2}(\partial T \setminus \partial \Omega)}^{2} + h_{T}^{\alpha + 2 - d} |\mathbf{F}|^{2} \chi(\{z \in T\}) \right)^{\frac{1}{2}},$$

$$(35)$$

where  $(\mathbf{u}_{\mathcal{T}}, p_{\mathcal{T}})$  denotes the solution to the discrete problem (26),  $\mathbf{I} \in \mathbb{R}^{d \times d}$  denotes the identity matrix, and the function  $\chi(\{z \in T\})$  equals one if  $z \in T$  and zero otherwise. Here we must recall that we consider our elements T to be closed sets. For a discrete tensor valued function  $\mathbf{W}_{\mathcal{T}}$ , we denote by  $[\![\mathbf{W}_{\mathcal{T}} \cdot \mathbf{v}]\!]$  the jump or interelement residual, which is defined, on the internal side  $S \in \mathcal{S}$  shared by the distinct elements  $T^+$ ,  $T^- \in \mathcal{N}_S$ , by

$$[\![\mathbf{W}_{\mathscr{T}} \cdot \mathbf{v}]\!] = \mathbf{W}_{\mathscr{T}|_{T^+}} \cdot \mathbf{v}^+ + \mathbf{W}_{\mathscr{T}|_{T^-}} \cdot \mathbf{v}^-. \tag{36}$$

Here  $v^+$ ,  $v^-$  are unit normals on S pointing towards  $T^+$ ,  $T^-$ , respectively. The error estimator is thus defined as

$$\mathscr{E}_{\alpha}(\mathbf{u}_{\mathscr{T}}, p_{\mathscr{T}}; \mathscr{T}) := \left(\sum_{T \in \mathscr{T}} \mathscr{E}_{\alpha}^{2}(\mathbf{u}_{\mathscr{T}}, p_{\mathscr{T}}; T)\right)^{\frac{1}{2}}.$$
(37)

#### 4.5. Error and residual

An important ingredient in the analysis that we will provide below is the so-called *residual*. Let  $(\mathbf{u}, p) \in \mathcal{X}$  and  $(\mathbf{u}_{\mathcal{T}}, p_{\mathcal{T}}) \in \mathbf{V}(\mathcal{T}) \times \mathcal{P}(\mathcal{T})$  denote the unique solutions to problems (13) and (26), respectively. In order to obtain information about the error  $(\mathbf{e}_{\mathbf{u}}, e_p) = (\mathbf{u} - \mathbf{u}_{\mathcal{T}}, p - p_{\mathcal{T}}) \in \mathcal{X}$ , we define the residual  $\mathcal{R} = \mathcal{R}(\mathbf{u}_{\mathcal{T}}, p_{\mathcal{T}}) \in \mathcal{Y}'$  as follows:

$$\langle \mathcal{R}, (\mathbf{v}, q) \rangle_{\mathcal{V}' \times \mathcal{V}} = \langle \mathbf{F} \delta_{\tau}, \mathbf{v} \rangle - c((\mathbf{u}_{\mathscr{T}}, p_{\mathscr{T}}), (\mathbf{v}, q)),$$
 (38)

where  $\langle \cdot, \cdot \rangle$  denotes the duality pairing between  $\mathbf{H}_0^1(\mathbf{d}_z^{-\alpha}, \Omega)'$  and  $\mathbf{H}_0^1(\mathbf{d}_z^{-\alpha}, \Omega)$  and the bilinear form c is defined in (14). Notice that the residual  $\mathcal{R}$  depends only on the data and the approximate solution  $(\mathbf{u}_{\mathscr{T}}, p_{\mathscr{T}})$  and is related to the error function by the relation

$$\langle \mathcal{R}, (\mathbf{v}, q) \rangle_{\mathcal{V}, \mathcal{V}} = c((\mathbf{e}_{\mathbf{u}}, e_p), (\mathbf{v}, q)) \quad \forall (\mathbf{v}, q) \in \mathcal{Y}.$$
 (39)

The following result shows that the  $\mathcal{Y}'$ -norm of  $\mathcal{R}$  is equivalent to the error.

**Lemma 6** (Abstract a Posteriori Error Bounds). If  $\alpha \in (d-2, d)$ , then

$$\beta \|(\mathbf{e}_{\mathbf{u}}, e_p)\|_{\mathcal{X}} \le \|\mathcal{R}\|_{\mathcal{Y}'} \le \|c\| \|(\mathbf{e}_{\mathbf{u}}, e_p)\|_{\mathcal{X}},\tag{40}$$

where  $\beta$  and  $\|c\|$  are the inf–sup and continuity constants of the bilinear form c, which are defined in (15) and (18), respectively, and verify  $0 < \beta \le \|c\|$ .

**Proof.** An application of the inf–sup condition (18), combined with the definition of the residual  $\mathcal{R}$  and the relation (39), imply that

$$\begin{split} \beta \| (\mathbf{e_u}, e_p) \|_{\mathcal{X}} &\leq \sup_{(\mathbf{0}, 0) \neq (\mathbf{v}, q) \in \mathcal{Y}} \frac{c((\mathbf{e_u}, e_p), (\mathbf{v}, q))}{\| (\mathbf{v}, q) \|_{\mathcal{Y}}} \\ &= \sup_{(\mathbf{0}, 0) \neq (\mathbf{v}, q) \in \mathcal{Y}} \frac{\langle \mathcal{R}, (\mathbf{v}, q) \rangle_{\mathcal{Y}', \mathcal{Y}}}{\| (\mathbf{v}, q) \|_{\mathcal{Y}}} = \| \mathcal{R} \|_{\mathcal{Y}'}. \end{split}$$

On the other hand,

$$\|\mathcal{R}\|_{\mathcal{Y}'} = \sup_{(\mathbf{0},0) \neq (\mathbf{v},q) \in \mathcal{Y}} \frac{c((\mathbf{e}_{\mathbf{u}}, e_p), (\mathbf{v}, q))}{\|(\mathbf{v}, q)\|_{\mathcal{Y}}} \le \|c\| \|(\mathbf{e}_{\mathbf{u}}, e_p)\|_{\mathcal{X}}. \tag{41}$$

Estimate (40) follows by collecting these two bounds.  $\Box$ 

### 4.5.1. Reliability

In what follows we obtain a global reliability property for the a posteriori error estimator (37).

**Theorem 7** (*Reliability*). Let  $(\mathbf{u}, p) \in \mathcal{X}$  be the unique solution to problem (13) and  $(\mathbf{u}_{\mathcal{T}}, p_{\mathcal{T}}) \in \mathbf{V}(\mathcal{T}) \times \mathcal{P}(\mathcal{T})$  its finite element approximation given as the solution to (26). If  $\alpha \in (d-2, d)$ , then

$$\|\nabla \mathbf{e}_{\mathbf{u}}\|_{L^{2}(\mathbf{d}^{\alpha}_{z},\Omega)} + \|e_{p}\|_{L^{2}(\mathbf{d}^{\alpha}_{z},\Omega)} \lesssim \mathcal{E}_{\alpha}(\mathbf{u}_{\mathscr{T}}, p_{\mathscr{T}}; \mathscr{T}),\tag{42}$$

where the hidden constant is independent of the continuous and discrete solutions, the size of the elements in the mesh  $\mathcal{T}$  and  $\#\mathcal{T}$ .

**Proof.** In view of the first bound in (40), we conclude that, to bound the  $\mathcal{X}$ -norm of the error, it suffices to control the dual norm  $\|\mathcal{R}\|_{\mathcal{Y}'}$ . To accomplish this task, we proceed as follows. Let  $(\mathbf{v}, q) \in \mathcal{Y}$  be arbitrary. Applying a standard

integration by parts argument to (38) yields

$$\langle \mathcal{R}, (\mathbf{v}, q) \rangle_{\mathcal{Y}', \mathcal{Y}} = \langle \mathbf{F} \delta_z, \mathbf{v} \rangle - c((\mathbf{u}_{\mathscr{T}}, p_{\mathscr{T}}), (\mathbf{v}, q)) = \langle \mathbf{F} \delta_z, \mathbf{v} \rangle$$

$$+ \sum_{T \in \mathscr{T}} \int_T (\Delta \mathbf{u}_{\mathscr{T}} - \nabla p_{\mathscr{T}}) \cdot \mathbf{v} - \sum_{S \in \mathscr{S}} \int_S [[(\nabla \mathbf{u}_{\mathscr{T}} - p_{\mathscr{T}} \mathbf{I}) \cdot \mathbf{v}]] \cdot \mathbf{v} - \sum_{T \in \mathscr{T}} \int_T q \operatorname{div} \mathbf{u}_{\mathscr{T}}.$$

$$(43)$$

Next we observe that, since  $V(\mathcal{T}) \times \mathcal{P}(\mathcal{T}) \subset \mathcal{Y}$ , we can invoke Galerkin orthogonality to conclude that, for all  $(\mathbf{v}_{\mathcal{T}}, q_{\mathcal{T}}) \in V(\mathcal{T}) \times \mathcal{P}(\mathcal{T})$ ,

$$0 = c((\mathbf{u} - \mathbf{u}_{\mathscr{T}}, p - p_{\mathscr{T}}), (\mathbf{v}_{\mathscr{T}}, q_{\mathscr{T}})) = \langle \mathbf{F} \delta_{z}, \mathbf{v}_{\mathscr{T}} \rangle - c((\mathbf{u}_{\mathscr{T}}, p_{\mathscr{T}}), (\mathbf{v}_{\mathscr{T}}, q_{\mathscr{T}})). \tag{44}$$

We now invoke the restriction operator  $\mathcal{Q}_{\mathscr{T}}$ , defined in (34), and set  $(\mathbf{v}_{\mathscr{T}}, 0) = \mathcal{Q}_{\mathscr{T}}(\mathbf{v}, q)$  in (44). By replacing the obtained relation into (43) we arrive at

$$\langle \mathcal{R}, (\mathbf{v}, q) \rangle_{\mathcal{Y}', \mathcal{Y}} = \langle \mathbf{F} \delta_z, \mathbf{v} - \mathbf{v}_{\mathscr{T}} \rangle + \sum_{T \in \mathscr{T}} \int_T (\Delta \mathbf{u}_{\mathscr{T}} - \nabla p_{\mathscr{T}}) \cdot (\mathbf{v} - \mathbf{v}_{\mathscr{T}}) - \sum_{S \in \mathscr{S}} \int_S [\![ (\nabla \mathbf{u}_{\mathscr{T}} - p_{\mathscr{T}} \mathbf{I}) \cdot \mathbf{v} ]\!] \cdot (\mathbf{v} - \mathbf{v}_{\mathscr{T}}) - \sum_{T \in \mathscr{T}} \int_T q \operatorname{div} \mathbf{u}_{\mathscr{T}} =: \mathbf{I} + \mathbf{II} - \mathbf{III} - \mathbf{IV}.$$

$$(45)$$

In what follows we proceed to control each term separately.

To bound II, we invoke the interpolation error estimate (30) and conclude that

$$II \lesssim \sum_{T \in \mathscr{T}} h_T D_T^{\frac{\alpha}{2}} \|\Delta \mathbf{u}_{\mathscr{T}} - \nabla p_{\mathscr{T}}\|_{\mathbf{L}^2(T)} \|\nabla \mathbf{v}\|_{\mathbf{L}^2(\mathsf{d}_z^{-\alpha}, \mathcal{S}_T)}. \tag{46}$$

We now proceed to control the term III. To accomplish this task, we apply the estimate (31) and arrive at

$$\operatorname{III} \lesssim \sum_{S \in \mathscr{S}} h_T^{\frac{1}{2}} D_T^{\frac{\alpha}{2}} \| \llbracket (\nabla \mathbf{u}_{\mathscr{T}} - p_{\mathscr{T}} \mathbf{I}) \cdot \mathbf{v} \rrbracket \|_{\mathbf{L}^2(S)} \| \nabla \mathbf{v} \|_{\mathbf{L}^2(\mathsf{d}_z^{-\alpha}, \mathcal{S}_T)}. \tag{47}$$

The control of the term IV follows from a simple application of the Cauchy–Schwarz inequality. In fact, we have

$$II \lesssim \sum_{T \in \mathscr{T}} \|\operatorname{div} \mathbf{u}_{\mathscr{T}}\|_{L^{2}(\mathsf{d}_{z}^{\alpha},T)} \|q\|_{L^{2}(\mathsf{d}_{z}^{-\alpha},T)}. \tag{48}$$

Since  $\mathbf{v} - \mathbf{v}_{\mathscr{T}} \in \mathbf{H}_0^1(\mathbf{d}_z^{-\alpha}, \Omega)$ , we control the term I by using the estimate of [13, Theorem 4.7] followed by the interpolation error estimate (29) and the local stability bound (28). These arguments allow us to conclude that

$$\langle \mathbf{F}\delta_{z}, \mathbf{v} - \mathbf{v}_{\mathscr{T}} \rangle \lesssim |\mathbf{F}| h_{T}^{\frac{\alpha}{2} - \frac{d}{2}} \|\mathbf{v} - \mathbf{v}_{\mathscr{T}}\|_{\mathbf{L}^{2}(\mathbf{d}_{z}^{-\alpha}, T)}$$

$$+ |\mathbf{F}| h_{T}^{\frac{\alpha}{2} + 1 - \frac{d}{2}} \|\nabla(\mathbf{v} - \mathbf{v}_{\mathscr{T}})\|_{\mathbf{L}^{2}(\mathbf{d}_{z}^{-\alpha}, T)}$$

$$\lesssim |\mathbf{F}| h_{T}^{\frac{\alpha}{2} + 1 - \frac{d}{2}} \|\nabla \mathbf{v}\|_{\mathbf{L}^{2}(\mathbf{d}_{z}^{-\alpha}, \mathcal{S}_{T})}.$$

$$(49)$$

Finally, by gathering the estimates for the terms I, II, III, and IV, obtained in (46)–(49), and resorting to the finite overlapping property of stars we arrive at the global upper bound (42) and conclude the proof.  $\Box$ 

### 4.5.2. Local efficiency

To derive efficiency properties of the local error indicator  $\mathcal{E}_{\alpha}(\mathbf{u}_{\mathcal{T}}, p_{\mathcal{T}}; T)$ , defined in (35), we utilize the standard residual estimation techniques developed in references [26,27] but on the basis of suitable bubble functions, whose construction we owe to [13, Section 5.2] and proceed to describe in what follows.

Given  $T \in \mathcal{T}$ , we first introduce a bubble function  $\varphi_T$  that satisfies the following properties:  $0 \le \varphi_T \le 1$ ,

$$\varphi_T(z) = 0, \qquad |T| \lesssim \int_T \varphi_T, \qquad \|\nabla \varphi_T\|_{L^{\infty}(R_T)} \lesssim h_T^{-1}, \tag{50}$$

and there exists a simplex  $T^* \subset T$  such that  $R_T := \text{supp}(\varphi_T) \subset T^*$ . Notice that, since  $\varphi_T$  satisfies (50), we have that

$$\|\theta\|_{L^2(R_T)} \lesssim \|\varphi_T^{\frac{1}{2}}\theta\|_{L^2(R_T)} \quad \forall \theta \in \mathbb{P}_2(R_T). \tag{51}$$

Second, given  $S \in \mathcal{S}$ , we introduce a bubble function  $\varphi_S$  that satisfies the following properties:  $0 \le \varphi_S \le 1$ ,

$$\varphi_S(z) = 0, \qquad |S| \lesssim \int_S \varphi_S, \qquad \|\nabla \varphi_S\|_{L^{\infty}(R_S)} \lesssim h_T^{-1/2} |S|^{1/2},$$
(52)

and  $R_S := \operatorname{supp}(\varphi_S)$  is such that, if  $\mathcal{N}_S = \{T, T'\}$ , there are simplices  $T_* \subset T$  and  $T'_* \subset T'$  such that  $R_S \subset T_* \cup T'_* \subset \mathcal{N}_S$ .

The following estimates that involve the bubble functions  $\varphi_T$  and  $\varphi_S$  are instrumental in the efficiency analysis that we will perform.

**Proposition 8** (Estimates for Bubble Functions). Let  $T \in \mathcal{T}$  and  $\varphi_T$  be the bubble function that satisfies (50). If  $\alpha \in (0, d)$ , then

$$h_T \|\nabla(\theta \varphi_T)\|_{L^2(\mathsf{d}_\tau^{-\alpha}, T)} \lesssim D_T^{-\frac{\alpha}{2}} \|\theta\|_{L^2(T)} \quad \forall \theta \in \mathbb{P}_2(T). \tag{53}$$

Let  $S \in \mathcal{S}$  and  $\varphi_S$  be the bubble function that satisfies (52). If  $\alpha \in (0, d)$ , then

$$h_T^{\frac{1}{2}} \|\nabla(\theta \varphi_S)\|_{L^2(\mathsf{d}_{-}^{-\alpha} \mathcal{N}_C)} \lesssim D_T^{-\frac{\alpha}{2}} \|\theta\|_{L^2(S)} \quad \forall \theta \in \mathbb{P}_3(S), \tag{54}$$

where  $\theta$  is extended to  $\mathcal{N}_S$  as a constant along the direction of one side of each element of  $\mathcal{T}$  contained in  $\mathcal{N}_S$ .

**Proof.** See [13, Lemma 5.2].  $\square$ 

The following result provides a local estimate for the residual  $\mathcal{R}$ .

**Lemma 9** (Local Dual Norm). Let G be a subdomain of  $\Omega$ . If  $\alpha \in (d-2,d)$ , then

$$\|\mathcal{R}\|_{\mathcal{V}'(G)} \lesssim \|(\mathbf{e}_{\mathbf{u}}, e_{n})\|_{\mathcal{X}(G)},\tag{55}$$

where the hidden constant is independent of  $(\mathbf{e}_{\mathbf{u}}, e_{p})$ .

**Proof.** Let  $(\mathbf{v}, q) \in \mathcal{Y}(G)$ . The extension of  $\mathbf{v}$  and q by zero to  $\Omega \setminus G$  yields functions  $(\tilde{\mathbf{v}}, \tilde{q}) \in \mathcal{Y}$ . We thus have that  $\langle \mathcal{R}, (\tilde{\mathbf{v}}, \tilde{q}) \rangle_{\mathcal{Y}, \mathcal{Y}} = c((\mathbf{e_u}, e_p), (\tilde{\mathbf{v}}, \tilde{q})) \lesssim \|(\mathbf{e_u}, e_p)\|_{\mathcal{X}(G)} \|(\mathbf{v}, q)\|_{\mathcal{Y}(G)}$ .

Consequently (55) follows. This concludes the proof.  $\Box$ 

With all these ingredients at hand, we are ready to derive the local efficiency properties of the local error indicator  $\mathscr{E}_{\alpha}(\mathbf{u}_{\mathscr{T}}, p_{\mathscr{T}}; T)$ .

**Theorem 10** (Local Efficiency). Let  $(\mathbf{u}, p) \in \mathcal{X}$  be the unique solution to problem (13) and  $(\mathbf{u}_{\mathscr{T}}, p_{\mathscr{T}}) \in \mathbf{V}(\mathscr{T}) \times \mathcal{P}(\mathscr{T})$  its finite element approximation given as the solution to (26). If  $\alpha \in (d-2, d)$ , then

$$\mathscr{E}_{\alpha}^{2}(\mathbf{u}_{\mathscr{T}}, p_{\mathscr{T}}; T) \lesssim \|\nabla \mathbf{e}_{\mathbf{u}}\|_{\mathbf{L}^{2}(\mathbf{d}_{\alpha}^{\alpha}, \mathcal{N}_{T})}^{2} + \|e_{p}\|_{L^{2}(\mathbf{d}_{\alpha}^{\alpha}, \mathcal{N}_{T})}^{2}, \tag{56}$$

where the hidden constant is independent of the continuous and discrete solutions, the size of the elements in the mesh  $\mathcal{T}$  and  $\#\mathcal{T}$ .

**Proof.** We estimate each contribution in (35) separately.

We begin the proof by bounding, for  $T \in \mathcal{T}$ , the term  $h_T^2 D_T^{\alpha} \| \Delta \mathbf{u}_{\mathcal{T}} - \nabla p_{\mathcal{T}} \|_{\mathbf{L}^2(T)}^2$ . Define  $\phi_T := \varphi_T(\Delta \mathbf{u}_{\mathcal{T}} - \nabla p_{\mathcal{T}})$  and invoke (51) to conclude that

$$\|\Delta \mathbf{u}_{\mathscr{T}} - \nabla p_{\mathscr{T}}\|_{\mathbf{L}^{2}(T)}^{2} \lesssim \int_{R_{T}} |\Delta \mathbf{u}_{\mathscr{T}} - \nabla p_{\mathscr{T}}|^{2} \varphi_{T} \leq \int_{T} (\Delta \mathbf{u}_{\mathscr{T}} - \nabla p_{\mathscr{T}}) \cdot \boldsymbol{\phi}_{T}.$$

$$(57)$$

We now consider the relation (43) with  $(\mathbf{v}, q) = (\boldsymbol{\phi}_T, 0)$  and observe that  $\boldsymbol{\phi}_T(z) = \varphi_T(z)(\Delta \mathbf{u}_{\mathscr{T}} - \nabla p_{\mathscr{T}})(z) = 0$ . This allows us to conclude that

$$\int_{T} (\Delta \mathbf{u}_{\mathscr{T}} - \nabla p_{\mathscr{T}}) \cdot \boldsymbol{\phi}_{T} = \langle \mathcal{R}, (\boldsymbol{\phi}_{T}, 0) \rangle_{\mathcal{Y}', \mathcal{Y}} = c((\mathbf{e}_{\mathbf{u}}, e_{p}), (\boldsymbol{\phi}_{T}, 0))$$

$$\lesssim \left( \|\nabla \mathbf{e}_{\mathbf{u}}\|_{\mathbf{L}^{2}(\mathsf{d}_{z}^{\alpha}, T)}^{2} + \|e_{p}\|_{\mathbf{L}^{2}(\mathsf{d}_{z}^{\alpha}, T)}^{2} \right)^{\frac{1}{2}} \|\nabla \boldsymbol{\phi}_{T}\|_{\mathbf{L}^{2}(\mathsf{d}_{z}^{-\alpha}, T)}.$$
(58)

We now recall that  $\phi_T = \varphi_T(\Delta \mathbf{u}_{\mathcal{T}} - \nabla p_{\mathcal{T}})$  and utilize (53) to conclude that

$$\|\nabla \boldsymbol{\phi}_T\|_{\mathbf{L}^2(\mathbf{d}_{-}^{-\alpha},T)} \lesssim h_T^{-1} D_T^{-\frac{\alpha}{2}} \|\Delta \mathbf{u}_{\mathscr{T}} - \nabla p_{\mathscr{T}}\|_{\mathbf{L}^2(T)}.$$

Replacing this estimate into (58), and the obtained one in (57), allows us to write

$$h_T^2 D_T^{\alpha} \| \Delta \mathbf{u}_{\mathscr{T}} - \nabla p_{\mathscr{T}} \|_{\mathbf{L}^2(T)}^2 \lesssim \| \nabla \mathbf{e}_{\mathbf{u}} \|_{\mathbf{L}^2(\mathsf{d}^{\alpha}, T)}^2 + \| e_p \|_{L^2(\mathsf{d}^{\alpha}, T)}^2. \tag{59}$$

Let  $T \in \mathscr{T}$  and S be a side of T. In what follows we control the jump term  $h_T D_T^{\alpha} \| [\![ (\nabla \mathbf{u}_{\mathscr{T}} - p_{\mathscr{T}} \mathbf{I}) \cdot \mathbf{v} ]\!] \|_{\mathbf{L}^2(\partial T \setminus \partial \Omega)}^2$  in (35). To accomplish this task, we proceed by using similar arguments to the ones that lead to (59) but now utilizing the bubble function  $\varphi_S$ . In fact, the use of properties (52) yields

$$\| \llbracket (\nabla \mathbf{u}_{\mathscr{T}} - p_{\mathscr{T}} \mathbf{I}) \cdot \mathbf{v} \rrbracket \|_{\mathbf{L}^{2}(S)}^{2} \lesssim \int_{S} | \llbracket (\nabla \mathbf{u}_{\mathscr{T}} - p_{\mathscr{T}} \mathbf{I}) \cdot \mathbf{v} \rrbracket |^{2} \varphi_{S} = \int_{S} \llbracket (\nabla \mathbf{u}_{\mathscr{T}} - p_{\mathscr{T}} \mathbf{I}) \cdot \mathbf{v} \rrbracket \cdot \boldsymbol{\phi}_{S},$$

where  $\phi_S := \varphi_S[[(\nabla \mathbf{u}_{\mathscr{T}} - p_{\mathscr{T}}\mathbf{I}) \cdot \mathbf{v}]]$ . Now, set  $(\mathbf{v}, q) = (\phi_S, 0)$  in (43), and use that  $\phi_S(z) = 0$  and that  $R_S = \operatorname{supp}(\phi_S) \subset T_* \cup T'_* \subset \mathcal{N}_S$ , to conclude that

$$\begin{split} \int_{S} & [ [(\nabla \mathbf{u}_{\mathscr{T}} - p_{\mathscr{T}} \mathbf{I}) \cdot \mathbf{v} ] ] \cdot \boldsymbol{\phi}_{S} = \sum_{T \in \mathcal{N}_{S}} \int_{T} (\Delta \mathbf{u}_{\mathscr{T}} - \nabla p_{\mathscr{T}}) \cdot \boldsymbol{\phi}_{S} - \langle \mathcal{R}, (\boldsymbol{\phi}_{S}, 0) \rangle_{\mathcal{Y}', \mathcal{Y}} \\ &= \sum_{T \in \mathcal{N}_{S}} \int_{T} (\Delta \mathbf{u}_{\mathscr{T}} - \nabla p_{\mathscr{T}}) \cdot \boldsymbol{\phi}_{S} - c((\mathbf{e}_{\mathbf{u}}, e_{p}), (\boldsymbol{\phi}_{S}, 0)) \\ &\leq \sum_{T \in \mathcal{N}_{S}} \| \Delta \mathbf{u}_{\mathscr{T}} - \nabla p_{\mathscr{T}} \|_{\mathbf{L}^{2}(T)} \| \boldsymbol{\phi}_{S} \|_{\mathbf{L}^{2}(T)} \\ &+ \sum_{T \in \mathcal{N}_{S}} \left( \| \nabla \mathbf{e}_{\mathbf{u}} \|_{\mathbf{L}^{2}(\mathbf{d}_{z}^{\alpha}, T)}^{2} + \| e_{p} \|_{\mathbf{L}^{2}(\mathbf{d}_{z}^{\alpha}, T)}^{2} \right)^{\frac{1}{2}} \| \nabla \boldsymbol{\phi}_{S} \|_{\mathbf{L}^{2}(\mathbf{d}_{z}^{-\alpha}, T)}. \end{split}$$

The control of the first term on the right-hand side of the previous expression follows from the fact that  $\|\phi_S\|_{\mathbf{L}^2(T)} \approx |T|^{\frac{1}{2}}|S|^{-\frac{1}{2}}\|\phi_S\|_{\mathbf{L}^2(S)}$  while the bound of the second term follows from (54). These arguments reveal that

$$\int_{S} \left[ \left[ \left( \nabla \mathbf{u}_{\mathscr{T}} - p_{\mathscr{T}} \mathbf{I} \right) \cdot \mathbf{v} \right] \cdot \boldsymbol{\phi}_{S} \lesssim \sum_{T \in \mathcal{N}_{S}} \left\| \Delta \mathbf{u}_{\mathscr{T}} - \nabla p_{\mathscr{T}} \right\|_{\mathbf{L}^{2}(T)} |T|^{\frac{1}{2}} |S|^{-\frac{1}{2}} \left\| \boldsymbol{\phi}_{S} \right\|_{\mathbf{L}^{2}(S)} + \sum_{T \in \mathcal{N}_{S}} \left( \left\| \nabla \mathbf{e}_{\mathbf{u}} \right\|_{\mathbf{L}^{2}(\mathsf{d}_{z}^{\alpha}, T)}^{2} + \left\| e_{p} \right\|_{L^{2}(\mathsf{d}_{z}^{\alpha}, T)}^{2} \right)^{\frac{1}{2}} D_{T}^{-\frac{\alpha}{2}} h_{T}^{-\frac{1}{2}} \left\| \boldsymbol{\phi}_{S} \right\|_{\mathbf{L}^{2}(S)}, \tag{60}$$

which, in view of (59),  $|T|/|S| \approx h_T$ , and  $\phi_S = \varphi_S[[(\nabla \mathbf{u}_{\mathscr{T}} - p_{\mathscr{T}}\mathbf{I}) \cdot \mathbf{v}]]$  imply that

$$h_T D_T^{\alpha} \| \llbracket (\nabla \mathbf{u}_{\mathscr{T}} - p_{\mathscr{T}} \mathbf{I}) \cdot \mathbf{v} \rrbracket \|_{\mathbf{L}^2(S)}^2 \lesssim \sum_{T' \subset \mathcal{N}_S} \left( \| \nabla \mathbf{e}_{\mathbf{u}} \|_{\mathbf{L}^2(\mathsf{d}_z^{\alpha}, T')}^2 + \| e_p \|_{L^2(\mathsf{d}_z^{\alpha}, T')}^2 \right). \tag{61}$$

The control of the term  $\|\operatorname{div} \mathbf{u}_{\mathscr{T}}\|_{L^2(\mathsf{d}_z^\alpha,T)}^2$  follows easily from the mass conservation equation, that reads  $\operatorname{div} \mathbf{u} = 0$ . In fact, for  $T \in \mathscr{T}$ , we have that

$$\|\operatorname{div} \mathbf{u}_{\mathscr{T}}\|_{L^{2}(\mathsf{d}^{\alpha}_{+},T)}^{2} = \|\operatorname{div} \mathbf{e}_{\mathbf{u}}\|_{L^{2}(\mathsf{d}^{\alpha}_{+},T)}^{2} \lesssim \|\nabla \mathbf{e}_{\mathbf{u}}\|_{L^{2}(\mathsf{d}^{\alpha}_{+},T)}^{2}. \tag{62}$$

Finally, we control the term  $h_T^{\alpha+2-d}|\mathbf{F}|^2\chi(\{z\in T\})$ . Let  $T\in \mathscr{T}$ , and notice first that, if  $T\cap\{z\}=\emptyset$ , then the estimate (56) follows from (59), (61), and (62). If, on the other hand,  $T\cap\{z\}=\{z\}$ , then the element indicator  $\mathscr{E}_{\alpha}$  contains the term  $h_T^{\alpha+2-d}|\mathbf{F}|^2$ . To control this term we follow the arguments developed in the proof of

[13, Theorem 5.3] that yield the existence of a smooth function  $\eta$  such that

$$\eta(z) = 1, \quad \|\eta\|_{L^{\infty}(\Omega)} = 1, \quad \|\nabla\eta\|_{L^{\infty}(\Omega)} = h_T^{-1}, \quad \text{supp}(\eta) \subset \mathcal{N}_T.$$
 (63)

With the function  $\eta$  at hand, we define  $\mathbf{v}_{\eta} := \mathbf{F} \eta \in \mathbf{H}_{0}^{1}(\mathbf{d}_{\tau}^{-\alpha}, \Omega)$  and notice that

$$|\mathbf{F}|^{2} = \langle \mathbf{F}\delta_{z}, \mathbf{v}_{\eta} \rangle = c((\mathbf{u}, p), (\mathbf{v}_{\eta}, 0)) = c((\mathbf{e}_{\mathbf{u}}, e_{p}), (\mathbf{v}_{\eta}, 0)) + c((\mathbf{u}_{\mathscr{T}}, p_{\mathscr{T}}), (\mathbf{v}_{\eta}, 0))$$

$$\lesssim \left( \|\nabla \mathbf{e}_{\mathbf{u}}\|_{\mathbf{L}^{2}(\mathsf{d}_{z}^{\alpha}, \mathcal{N}_{T})}^{2} + \|e_{p}\|_{L^{2}(\mathsf{d}_{z}^{\alpha}, \mathcal{N}_{T})}^{2} \|\nabla \mathbf{v}_{\eta}\|_{\mathbf{L}^{2}(\mathsf{d}_{z}^{-\alpha}, \mathcal{N}_{T})} + \sum_{T' \in \mathscr{T}: T' \subset \mathcal{N}_{T}} \|\Delta \mathbf{u}_{\mathscr{T}} - \nabla p_{\mathscr{T}}\|_{\mathbf{L}^{2}(T')} \|\mathbf{v}_{\eta}\|_{\mathbf{L}^{2}(T')} + \sum_{T' \in \mathscr{T}: T' \subset \mathcal{N}_{T}} \sum_{S \in \mathscr{S}_{T'}: S \notin \partial \mathcal{N}_{T}} \| \| \|(\nabla \mathbf{u}_{\mathscr{T}} - p_{\mathscr{T}}\mathbf{I}) \cdot \mathbf{v} \|_{\mathbf{L}^{2}(S)} \|\mathbf{v}_{\eta}\|_{L^{2}(S)}.$$

$$(64)$$

We now use the estimates

$$\|\eta\|_{L^2(S)} \lesssim h_T^{\frac{d-1}{2}}, \quad \|\eta\|_{L^2(\mathcal{N}_T)} \lesssim h_T^{\frac{d}{2}}, \quad \|\nabla \eta\|_{L^2(\mathbf{d}_z^{-\alpha},\mathcal{N}_T)} \lesssim h_T^{\frac{d-2}{2}-\frac{\alpha}{2}},$$

to conclude that

$$|\mathbf{F}|^{2} \lesssim h_{T}^{\frac{d-2}{2} - \frac{\alpha}{2}} |\mathbf{F}| \left( \|\nabla \mathbf{e}_{\mathbf{u}}\|_{\mathbf{L}^{2}(\mathsf{d}_{z}^{\alpha}, \mathcal{N}_{T})}^{2} + \|e_{p}\|_{L^{2}(\mathsf{d}_{z}^{\alpha}, \mathcal{N}_{T})}^{2} \right)^{\frac{1}{2}}$$

$$+ h_{T}^{\frac{d-2}{2} - \frac{\alpha}{2}} |\mathbf{F}| \left( \sum_{T' \in \mathcal{T}: T' \subset \mathcal{N}_{T}} h_{T'} D_{T'}^{\frac{\alpha}{2}} \|\Delta \mathbf{u}_{\mathcal{T}} - \nabla p_{\mathcal{T}}\|_{\mathbf{L}^{2}(T')} \right)$$

$$+ \sum_{T' \in \mathcal{T}: T' \subset \mathcal{N}_{T'}} \sum_{S \in \mathcal{S}_{T}: S \notin \partial \mathcal{N}_{T}} D_{T'}^{\frac{\alpha}{2}} h_{T'}^{\frac{1}{2}} \| [\![ (\nabla \mathbf{u}_{\mathcal{T}} - p_{\mathcal{T}} \mathbf{I}) \cdot \mathbf{v} ]\!] \|_{L^{2}(S)} \right),$$

$$(65)$$

where we have also used that, since  $z \in T$ ,  $h_T \approx D_T$ . Use the estimates (59) and (61) and conclude.  $\square$ 

## 5. Low order stabilized schemes

In the previous section we have provided an a posteriori error analysis for the discrete scheme (26) that is based on the finite element pairs (21)–(22) and (23)–(24). We recall that both of these pairs are compatible, i.e., they satisfy the discrete inf–sup condition (25), and that this feature does come at a cost. Namely, this condition requires to increase the polynomial degree of the discrete spaces beyond what is required for conformity: it is not possible to approximate the velocity field with piecewise linears, while the pressure space is approximated by piecewise constants or linears; see [1, Section 4.2.3]. If lowest order possible is desired, it is thus necessary to modify the discrete problem to circumvent the need of satisfying condition (25) [30]: this gives rise to the so-called *stabilized methods*. In the literature several stabilized techniques can be found: the residual-free-bubbles method, variational multiscale formulations, enriched Petrov–Galerkin methods, pressure projection methods, local projection techniques and Galerkin/least-squares formulations. For an extensive review of different stabilized finite element methods we refer the reader to [31, Part IV, Section 3], [32, Chapter 7], and [33, Chapter 4].

Let us now describe the low-order stabilized schemes that we shall consider. First we introduce the following finite element spaces

$$\mathbf{V}_{\text{stab}}(\mathscr{T}) = \left\{ \mathbf{v}_{\mathscr{T}} \in \mathbf{C}(\bar{\Omega}) : \forall T \in \mathscr{T}, \mathbf{v}_{\mathscr{T}}|_{T} \in \mathbb{P}_{1}(T)^{d} \right\} \cap \mathbf{H}_{0}^{1}(\Omega), \tag{66}$$

$$\mathcal{P}_{\ell,\text{stab}}(\mathcal{T}) = \left\{ q_{\mathcal{T}} \in L^2(\Omega)/\mathbb{R} : \ \forall T \in \mathcal{T}, q_{\mathcal{T}}|_T \in \mathbb{P}_{\ell}(T) \right\},\tag{67}$$

where  $\ell \in \{0, 1\}$ . The approximation to problem (13) seeks then a pair  $(\mathbf{u}_{\mathscr{T}}, p_{\mathscr{T}})$  in  $\mathbf{V}_{\text{stab}}(\mathscr{T}) \times \mathcal{P}_{\ell, \text{stab}}(\mathscr{T})$  such that

$$\begin{cases}
a(\mathbf{u}_{\mathcal{T}}, \mathbf{v}_{\mathcal{T}}) + b(\mathbf{v}_{\mathcal{T}}, p_{\mathcal{T}}) + s(\mathbf{u}_{\mathcal{T}}, \mathbf{v}_{\mathcal{T}}) = \mathbf{F} \cdot \mathbf{v}_{\mathcal{T}}(z), & \forall \mathbf{v}_{\mathcal{T}} \in \mathbf{V}_{\text{stab}}(\mathcal{T}), \\
-b(\mathbf{u}_{\mathcal{T}}, q_{\mathcal{T}}) + m(p_{\mathcal{T}}, q_{\mathcal{T}}) = 0, & \forall q_{\mathcal{T}} \in \mathcal{P}_{\ell,\text{stab}}(\mathcal{T}),
\end{cases}$$
(68)

where the bilinear forms  $s: \mathbf{V}_{\text{stab}}(\mathcal{T}) \times \mathbf{V}_{\text{stab}}(\mathcal{T}) \to \mathbb{R}$  and  $m: \mathcal{P}_{\ell,\text{stab}}(\mathcal{T}) \times \mathcal{P}_{\ell,\text{stab}}(\mathcal{T}) \to \mathbb{R}$  are chosen as in [31, Part IV, Section 3.1], and are meant to stabilize the scheme:

$$s(\mathbf{u}_{\mathscr{T}}, \mathbf{v}_{\mathscr{T}}) := \sum_{T \in \mathscr{T}} \tau_{\text{div}} \int_{T} \text{div } \mathbf{u}_{\mathscr{T}} \text{div } \mathbf{v}_{\mathscr{T}},$$

$$m(p_{\mathscr{T}}, q_{\mathscr{T}}) := \sum_{T \in \mathscr{T}} \tau_{T} \int_{T} \nabla p_{\mathscr{T}} \cdot \nabla q_{\mathscr{T}} + \sum_{S \in \mathscr{S}} \tau_{S} h_{S} \int_{S} \llbracket p_{\mathscr{T}} \rrbracket \llbracket q_{\mathscr{T}} \rrbracket,$$

$$(69)$$

where  $\tau_{\rm div} \geq 0$ ,  $\tau_T \geq 0$  and  $\tau_S > 0$  denote the so-called stabilization parameters, and  $[q_{\mathscr{T}}]$  has a similar meaning as in the tensor valued case described in (36). It follows from [31, Lemma 3.4, Section 3.1] (when  $\tau_T > 0$ ) and [34, Section 2.1] (when  $\tau_T = 0$  and  $\ell = 0$ ) that problem (68) is well-posed.

We immediately notice that, due to the presence of the stabilization terms s and m in the discrete problem (68), the Galerkin orthogonality property (44) is no longer valid. Instead, we have the relation

$$\langle \mathcal{R}, (\mathbf{v}_{\mathscr{T}}, q_{\mathscr{T}}) \rangle_{\mathcal{V}', \mathcal{V}} = s(\mathbf{u}_{\mathscr{T}}, \mathbf{v}_{\mathscr{T}}) + m(p_{\mathscr{T}}, q_{\mathscr{T}}) \quad \forall (\mathbf{v}_{\mathscr{T}}, q_{\mathscr{T}}) \in \mathbf{V}_{\text{stab}}(\mathscr{T}) \times \mathcal{P}_{\ell, \text{stab}}(\mathscr{T}),$$

where  $\mathcal{R}$  is defined in (38). The previous relation can be rewritten, for  $(\mathbf{v}_{\mathscr{T}}, q_{\mathscr{T}}) \in \mathbf{V}_{\text{stab}}(\mathscr{T}) \times \mathcal{P}_{\ell,\text{stab}}(\mathscr{T})$ , as

$$0 = \langle \mathbf{F}\delta_z, \mathbf{v}_{\mathscr{T}} \rangle - c((\mathbf{u}_{\mathscr{T}}, p_{\mathscr{T}}), (\mathbf{v}_{\mathscr{T}}, q_{\mathscr{T}})) - s(\mathbf{u}_{\mathscr{T}}, \mathbf{v}_{\mathscr{T}}) - m(p_{\mathscr{T}}, q_{\mathscr{T}}). \tag{70}$$

For the discrete scheme (68), we define the local error indicators

$$\begin{split} \mathcal{E}_{\alpha, \text{stab}}(\mathbf{u}_{\mathscr{T}}, \, p_{\mathscr{T}}; \, T) &\coloneqq \left( h_T^2 D_T^{\alpha} \| \Delta \mathbf{u}_{\mathscr{T}} - \nabla p_{\mathscr{T}} \|_{\mathbf{L}^2(T)}^2 + (1 + \tau_{\text{div}}^2) \| \operatorname{div} \mathbf{u}_{\mathscr{T}} \|_{\mathbf{L}^2(\mathbf{d}_z^{\alpha}, T)}^2 \right. \\ &\quad + h_T D_T^{\alpha} \| \left[ \left[ (\nabla \mathbf{u}_{\mathscr{T}} - p_{\mathscr{T}} \mathbf{I}) \cdot \mathbf{v} \right] \right] \|_{\mathbf{L}^2(\partial T \setminus \partial \Omega)}^2 + h_T^{\alpha + 2 - d} |\mathbf{F}|^2 \chi(\{z \in T\}) \right)^{\frac{1}{2}}, \end{split}$$

and the global error estimator

$$\mathcal{E}_{\alpha,\text{stab}}(\mathbf{u}_{\mathscr{T}}, p_{\mathscr{T}}; \mathscr{T}) := \left(\sum_{T \in \mathscr{T}} \mathcal{E}_{\alpha,\text{stab}}^{2}(\mathbf{u}_{\mathscr{T}}, p_{\mathscr{T}}; T)\right)^{\frac{1}{2}}.$$
(71)

It is now our intention to show the reliability and efficiency of this estimator.

**Theorem 11** (Reliability and Local Efficiency). Let the pair  $(\mathbf{u}, p) \in \mathbf{H}_0^1(\mathsf{d}_z^{\alpha}, \Omega) \times L^2(\mathsf{d}_z^{\alpha}, \Omega)/\mathbb{R}$  be the solution to problem (13) and  $(\mathbf{u}_{\mathscr{T}}, p_{\mathscr{T}}) \in \mathbf{V}_{\text{stab}}(\mathscr{T}) \times \mathcal{P}_{\ell,\text{stab}}(\mathscr{T})$  its stabilized finite element approximation given as the solution to (68). If  $\alpha \in (d-2, d)$ , then

$$\|\nabla \mathbf{e}_{\mathbf{u}}\|_{\mathbf{L}^{2}(\mathsf{d}_{z}^{\alpha},\Omega)}^{2} + \|e_{p}\|_{L^{2}(\mathsf{d}_{z}^{\alpha},\Omega)}^{2} \lesssim \mathcal{E}_{\alpha,\mathsf{stab}}^{2}(\mathbf{u}_{\mathscr{T}},p_{\mathscr{T}};\mathscr{T}),\tag{72}$$

and

$$\mathcal{E}_{\alpha,\text{stab}}^{2}(\mathbf{u}_{\mathscr{T}}, p_{\mathscr{T}}; T) \lesssim \|\nabla \mathbf{e}_{\mathbf{u}}\|_{\mathbf{L}^{2}(\mathbf{d}_{\tau}^{\alpha}, \mathcal{N}_{T})}^{2} + \|e_{p}\|_{L^{2}(\mathbf{d}_{\tau}^{\alpha}, \mathcal{N}_{T})}^{2}, \tag{73}$$

where the hidden constants in both inequalities are independent of the continuous and discrete solutions, the size of the elements in the mesh  $\mathcal{T}$  and  $\#\mathcal{T}$ .

**Proof.** Let  $(\mathbf{v}, q) \in \mathcal{Y}$ . We invoke the restriction operator  $\mathcal{Q}_{\mathscr{T}}$ , defined in (34), and set  $(\mathbf{v}_{\mathscr{T}}, 0) = \mathcal{Q}_{\mathscr{T}}(\mathbf{v}, q)$  in (70), to conclude that

$$\begin{split} \langle \mathcal{R}, (\mathbf{v}, q) \rangle_{\mathcal{Y}, \mathcal{Y}} &= \langle \mathbf{F} \delta_z, \mathbf{v} - \mathbf{v}_{\mathcal{T}} \rangle + \sum_{T \in \mathcal{T}} \int_T (\Delta \mathbf{u}_{\mathcal{T}} - \nabla p_{\mathcal{T}}) \cdot (\mathbf{v} - \mathbf{v}_{\mathcal{T}}) \\ &- \sum_{S \in \mathcal{S}} \int_S \llbracket (\nabla \mathbf{u}_{\mathcal{T}} - p_{\mathcal{T}} \mathbf{I}) \cdot \mathbf{v} \rrbracket \cdot (\mathbf{v} - \mathbf{v}_{\mathcal{T}}) - \sum_{T \in \mathcal{T}} q \operatorname{div} \mathbf{u}_{\mathcal{T}} + s(\mathbf{u}_{\mathcal{T}}, \mathbf{v}_{\mathcal{T}}). \end{split}$$

Notice that the first four terms on the right-hand side of the previous expression have been previously controlled; see the estimates (46)–(49). It is thus sufficient to control the last term. To bound it we invoke the local stability

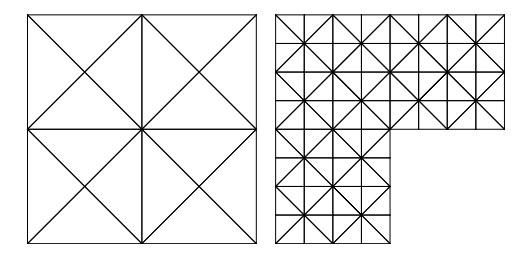


Fig. 1. The initial meshes  $\mathcal{T}_0$  used in the adaptive Algorithm 1 when  $\Omega$  is a square (left) and a two-dimensional L-shaped domain (right).

property (28) of the quasi-interpolation operator  $\Pi_{\mathscr{T}}$  to conclude that

$$|s(\mathbf{u}_{\mathscr{T}}, \Pi_{\mathscr{T}}\mathbf{v})| \leq \sum_{T \in \mathscr{T}} \tau_{\text{div}} \int_{T} |\operatorname{div} \mathbf{u}_{\mathscr{T}} \operatorname{div} \Pi_{\mathscr{T}}\mathbf{v}|$$

$$\lesssim \sum_{T \in \mathscr{T}} \tau_{\text{div}} \|\operatorname{div} \mathbf{u}_{\mathscr{T}}\|_{L^{2}(\mathsf{d}_{z}^{\alpha}, T)} \|\nabla \mathbf{v}\|_{L^{2}(\mathsf{d}_{z}^{-\alpha}, \mathcal{S}_{T})}.$$

Consequently, invoking the finite overlapping property of stars, we arrive at

$$|s(\mathbf{u}_{\mathscr{T}}, \mathbf{v}_{\mathscr{T}})| \leq \|\nabla \mathbf{v}\|_{L^{2}(\mathbf{d}_{z}^{-\alpha}, \Omega)} \left( \sum_{T \in \mathscr{T}} \tau_{\mathrm{div}}^{2} \|\operatorname{div} \mathbf{u}_{\mathscr{T}}\|_{L^{2}(\mathbf{d}_{z}^{\alpha}, T)}^{2} \right)^{\frac{1}{2}}.$$

Finally, by gathering the estimates (46)–(49) with the previous one, and resorting to the finite overlapping property of stars, again, we arrive at the global upper bound (72).

The local efficiency (73) follows as a direct consequence of the estimate in Theorem 10 since, as it is usual in residual error estimation, the lower bound does not contain any consistency terms, even when stabilized schemes are considered; see [26].  $\Box$ 

### 6. Numerical experiments

In this section we present a series of numerical examples that illustrate the performance of the devised error estimators  $\mathcal{E}_{\alpha}$  and  $\mathcal{E}_{\alpha,\text{stab}}$ . To explore the performance of  $\mathcal{E}_{\alpha}$ , defined in (37), we consider the discrete problem (26) with the discrete spaces (23)–(24). This setting will be referred to as *Taylor–Hood approximation*. The performance of the estimator  $\mathcal{E}_{\alpha,\text{stab}}$ , defined in (71), will be explored with the following finite element setting: the discrete spaces are (66) and (67), with  $\ell = 0$ , and the stabilization parameters are  $\tau_{\text{div}} = 0$ ,  $\tau_T = 0$ , and  $\tau_S = 1/12$ . This setting will be referred to as *low-order stabilized approximation*.

The numerical experiments that will be presented have been carried out with the help of a code that we implemented using C++. All matrices have been assembled exactly and the global linear systems were solved using the multifrontal massively parallel sparse direct solver (MUMPS) [35,36]. The right hand sides and terms involving the weight, and the approximation errors, are computed by a quadrature formula which is exact for polynomials of degree 19. After obtaining the approximate solution of (26) or (68), we calculate the local indicators  $\mathcal{E}_{\alpha}(\mathbf{u}_{\mathcal{T}}, p_{\mathcal{T}}; T)$  or  $\mathcal{E}_{\alpha,\text{stab}}(\mathbf{u}_{\mathcal{T}}, p_{\mathcal{T}}; T)$  to drive the adaptive mesh refinement procedures described in Algorithm 1 and the global a posteriori error estimator  $\mathcal{E}_{\alpha}$  or  $\mathcal{E}_{\alpha,\text{stab}}$  in order to assess the accuracy of the approximation. In this way, a sequence of adaptively refined meshes was generated from the initial meshes shown in Fig. 1. Notice that three different marking strategies are considered in Algorithm 1: the maximum, Dörfler [37], and average strategies.

We define the total number of degrees of freedom as Ndof :=  $\dim \mathfrak{W} + \dim \mathfrak{P}$ , where  $(\mathfrak{W}, \mathfrak{P}) = (V(\mathscr{T}), \mathcal{P}(\mathscr{T}))$  for the Taylor–Hood approximation, and  $(\mathfrak{W}, \mathfrak{P}) = (V_{\text{stab}}(\mathscr{T}), \mathcal{P}_{\ell,\text{stab}}(\mathscr{T}))$  in the low-order stabilized setting. We measure experimental rates of convergence for the error in the  $\mathcal{X}$ -norm, that is

$$\|(\boldsymbol{e}_{\mathbf{u}}, \boldsymbol{e}_{p})\|_{\mathcal{X}} := \left(\|\nabla(\mathbf{u} - \mathbf{u}_{\mathscr{T}})\|_{\mathbf{L}^{2}(\mathsf{d}_{\tau}^{\alpha}, \Omega)}^{2} + \|p - p_{\mathscr{T}}\|_{\mathbf{L}^{2}(\mathsf{d}_{\tau}^{\alpha}, \Omega)}^{2}\right)^{\frac{1}{2}}.$$

$$(74)$$

## Algorithm 1 Adaptive Algorithm.

Input: Initial mesh  $\mathcal{I}_0$ , interior point  $z \in \Omega$ ,  $\alpha$ , and stabilization parameters;

- 1: Solve the discrete problem (26) ((68));
- **2:** For each  $T \in \mathcal{T}$  compute the local error indicator  $\mathcal{E}_{\alpha}(\mathbf{u}_{\mathcal{T}}, p_{\mathcal{T}}; T)$  ( $\mathcal{E}_{\alpha, \text{stab}}(\mathbf{u}_{\mathcal{T}}, p_{\mathcal{T}}; T)$ ) given as in (37) ((71));
- **3:** Mark an element  $T \in \mathcal{T}$  for refinement using either a:
  - Maximum strategy:  $\mathcal{E}_{\alpha}(\mathbf{u}_{\mathcal{T}}, p_{\mathcal{T}}; T)^2 \geq \frac{1}{2} \max_{T' \in \mathcal{T}} \mathcal{E}_{\alpha}(\mathbf{u}_{\mathcal{T}}, p_{\mathcal{T}}; T')^2$ .
  - Dörfler strategy: see [37].
  - Average strategy:  $\mathscr{E}_{\alpha}(\mathbf{u}_{\mathscr{T}}, p_{\mathscr{T}}; T)^2 \geq \frac{1}{\#\mathscr{T}} \sum_{T' \in \mathscr{T}} \mathscr{E}_{\alpha}(\mathbf{u}_{\mathscr{T}}, p_{\mathscr{T}}; T')^2$ .

Similar strategies are considered for  $\mathcal{E}_{\alpha,\text{stab}}(\mathbf{u}_{\mathcal{T}}, p_{\mathcal{T}}; T)$ ;

**4:** From step **3**, construct a new mesh, using a longest edge bisection algorithm. Set  $i \leftarrow i + 1$ , and go to step **1**.

#### 6.1. Standard a posteriori error estimator based on regularization

Before we even begin to illustrate the performance of our estimators, it is instructive to pause and ponder whether the development of a new error estimator is really warranted. To explore this we consider a few examples. We consider a discretization of problem (1) via the Taylor–Hood pair (23)–(24). This gives rise to problem (26). While this problem can be implemented without issues, if we wish to consider its a posteriori error estimation using, for instance, the residual based techniques of [26], we immediately face an issue. Namely, the right hand side is not in  $\mathbf{L}^2(\Omega)$ , it is not even an element of  $\mathbf{H}^{-1}(\Omega)$ . A suitable proxy for  $\mathbf{F}\delta_z$  must be constructed, or the estimator must be modified. If we follow the first route, suitable regularizations of the Dirac mass centered at  $z \in \Omega$  need to be considered. Following [38, Section 4.4.2], we consider

$$\delta_{z,a}^{1}(x) = \frac{1}{a\sqrt{\pi}} e^{-\frac{|x-z|^2}{a^2}}, \quad \delta_{z,a}^{2}(x) = \frac{a/\pi}{a^2 + |x-z|^2}, \quad a \in \mathbb{R}_+.$$
 (75)

Notice that for, i = 1,2, and any continuous function f it holds that

$$\lim_{a\downarrow 0} \int_{\mathbb{D}} \delta_{z,a}^{i}(x) f(x) = f(z).$$

Similarly, from [39, Section 3.3.1] we will also consider the following polynomial regularization, for  $a \in \mathbb{R}_+$ :

$$\delta_{z,a}^{3}(x) = \begin{cases} \frac{1}{a} \left( -30 \left( \frac{|x-z|}{a} \right)^{3} + 60 \left( \frac{|x-z|}{a} - 36 \frac{|x-z|}{a} + 6 \right)^{2} \right), & \text{if } |x-z| \le a, \\ 0, & \text{otherwise.} \end{cases}$$
 (76)

We can thus consider the following residual-type a posteriori error estimator [40]:

$$\mathcal{E}_{\mathrm{rg},\mathrm{i}}(\mathbf{u}_{\mathscr{T}},\,p_{\mathscr{T}};\,\mathscr{T})^2 = \sum_{T\in\mathscr{T}} \mathcal{E}_{\mathrm{rg},\mathrm{i}}(\mathbf{u}_{\mathscr{T}},\,p_{\mathscr{T}};\,T)^2,$$

based on the local indicators

$$\mathcal{E}_{rg,i}(\mathbf{u}_{\mathscr{T}}, p_{\mathscr{T}}; T)^{2} = h_{T}^{2} \left\| \mathbf{F} \delta_{z,a}^{i} + \Delta \mathbf{u}_{\mathscr{T}} - \nabla p_{\mathscr{T}} \right\|_{\mathbf{L}^{2}(T)}^{2} + \|\operatorname{div} \mathbf{u}_{\mathscr{T}}\|_{L^{2}(T)}^{2} + h_{T} \| \left\| \left[ \left( \nabla \mathbf{u}_{\mathscr{T}} - p_{\mathscr{T}} \mathbf{I} \right) \cdot \mathbf{v} \right] \right\|_{\mathbf{L}^{2}(\partial T \setminus \partial \Omega)}^{2}.$$

$$(77)$$

In Fig. 2 we present the experimental rates of convergence that we obtained when the adaptive procedure of Algorithm 1 is driven by the residual-type a posteriori error indicators defined in (77). We consider  $\delta_{z,a}^i$  as the regularizations given in (75) and (76) with different values of the constant a:  $a \in \{10^{-2}, 10^{-3}, 10^{-4}, 10^{-5}, 10^{-6}\}$ . From Fig. 2, it can be observed that for all the regularization techniques and the different values of a that we have considered, optimal convergence is not achieved.

Notice that, albeit suboptimally, the estimator seems to converge to zero. However, we believe this to be a preasymptotic phenomenon. As the estimator decreases to the scale of the parameter a, we expect one of either two things to happen. The estimator will either stagnate, as we are measuring the error in a space that does not contain

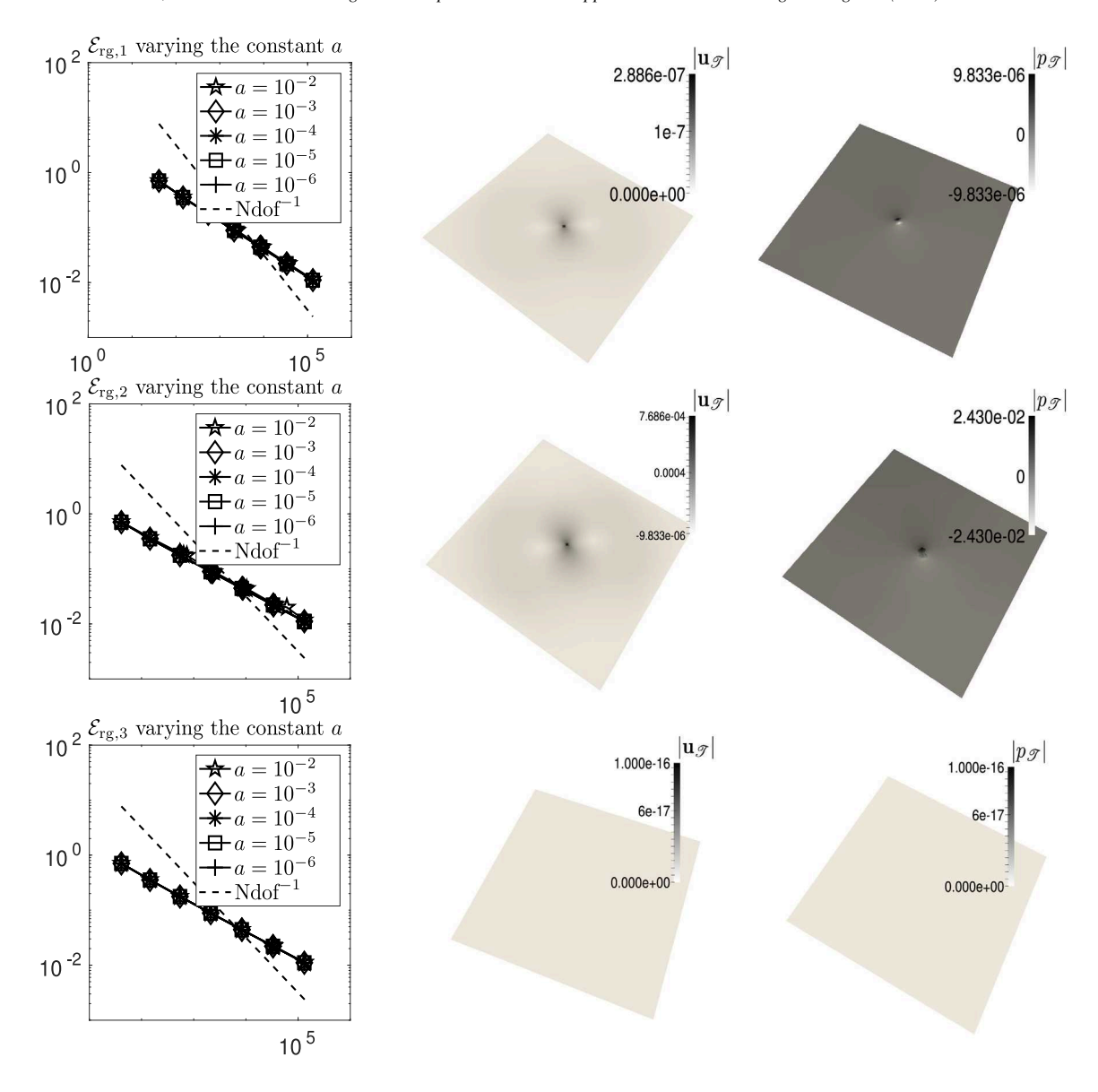


Fig. 2. Experimental rates of convergence for the residual-type error estimators  $\mathcal{E}_{\text{rg,i}}$  (maximum strategy) for  $i \in \{1, 2, 3\}$  and different values of the constant a:  $a \in \{10^{-2}, 10^{-3}, 10^{-4}, 10^{-5}, 10^{-6}\}$ . We also present the finite element solutions  $|\mathbf{u}_{\mathcal{T}}|$  and  $p_{\mathcal{T}}$  obtained for the value  $a = 10^{-4}$ , after six adaptive refinements, when the regularization  $\delta_{z,a}^1$  (middle), and  $\delta_{z,a}^3$  (bottom), respectively, is used.

the exact solution, or the estimator will converge to zero, but our numerical solution will not converge to the exact one. This seems consistent with the plots of the finite element solutions shown in Fig. 2. See also the experiment presented in Section 6.4 for an illustration further supporting this claim.

In conclusion, a naïve a posteriori error estimator does not achieve its goal in this class of problems and, consequently, all our developments are indeed necessary.

### 6.2. Convex and non-convex domains with homogeneous boundary conditions

We now explore the performance of our devised a posteriori error estimators in problems where no analytical solution is available: convex and non-convex domains  $\Omega$  are considered.

## 6.2.1. Example 1: Convex domain

We consider the square domain  $\Omega = (0, 1)^2$ ,  $\mathbf{F} = (1, 1)^T$ , and  $z = (0.5, 0.5)^T$ . We explore the performance of  $\mathcal{E}_{\alpha}$  (Taylor–Hood approximation) and  $\mathcal{E}_{\alpha,\text{stab}}$  (low-order stabilized approximation) when driving the adaptive procedures of Algorithm 1. We first investigate the effect of varying the exponent  $\alpha$  in the Muckenhoupt weight  $\mathbf{d}_z^{\alpha}$ , defined in (3), and explore the three marking strategies introduced in Algorithm 1. We consider

$$\alpha \in \{0.25, 0.5, 0.75, 1.25, 1.5, 1.75\}.$$

Second, for  $\alpha=1.0$ , we compare the performance of our adaptive algorithm with standard uniform refinement. We notice that the computation of the local error indicators and error estimators requires the use of a suitable integration rule. We explore the effect of quadrature by comparing the performance of the underlying AFEM with a quadrature formula that is exact for polynomials of degree 19 and another one that is based on composite integration: we subdivide each triangle into four by joining its midpoints.

In Fig. 3 we present the experimental rates of convergence for the error estimators  $\mathscr{E}_{\alpha}$  and  $\mathscr{E}_{\alpha,stab}$ . We observe that the three marking strategies of Algorithm 1 yield optimal experimental rates of convergence for all the values of the parameter  $\alpha$  that we considered. In Fig. 4 we observe, as expected, that the adaptive loop of Algorithm 1, when the maximum strategy is considered, outperforms standard uniform refinement. In Fig. 5 we show that optimal experimental rates of convergence for the error estimators are attained for both of the quadrature formulas previously mentioned. In Fig. 6, we present the results obtained by Algorithm 1 when is driven by the local indicators  $\mathscr{E}_{\alpha}$  and  $\mathscr{E}_{\alpha,stab}$  and the maximum strategy is considered. We show the finite element approximations of  $|\mathbf{u}_{\mathscr{T}}|$  and  $p_{\mathscr{T}}$  and the final meshes obtained by the aforementioned schemes. We observe that most of the adaptive refinement is concentrated around the delta source.

## 6.2.2. Example 2: L-shaped domain

We let  $\Omega = (-1, 1)^2 \setminus [0, 1) \times [-1, 0)$ , an L-shaped domain, set in (26) the data to be  $\mathbf{F} = (1, 1)^T$  and  $z = (0.5, 0.5)^T$ , and fix the exponent of the Muckenhoupt weight  $d_z^{\alpha}$  in (3) as  $\alpha = 1.5$ . In Figs. 7 and 8, we present the results obtained by Algorithm 1 when driven by the local indicators  $\mathcal{E}_{1.5}$  (Taylor–Hood approximation) and  $\mathcal{E}_{1.5,\text{stab}}$  (low-order stabilized approximation). For mesh refinement, we have considered the maximum strategy. We show, in Fig. 8, the finite element approximations of  $|\mathbf{u}_{\mathcal{T}}|$  and  $p_{\mathcal{T}}$  and the final meshes obtained by the aforementioned schemes. We also present the experimental rates of convergence rate for the estimators  $\mathcal{E}_{1.5}$  and  $\mathcal{E}_{1.5,\text{stab}}$ . We observe that optimal experimental rates of convergence are attained, and that most of the adaptive refinement is concentrated around the delta source. In Fig. 7, we present the experimental rate of convergence for the total error estimators  $\mathcal{E}_{\alpha}$  and  $\mathcal{E}_{\alpha,\text{stab}}$  when  $\alpha \in \{0.5, 0.75, 1, 1.25, 1.5\}$ . It can be observed that, for all the cases that we have considered, optimal rates of convergence are attained.

## 6.3. Example 3: A series of Dirac sources

We now go beyond the presented theory and include a series of Dirac delta sources on the right-hand side of the momentum equation. To be precise, we will replace the momentum equation in (1) by

$$-\Delta \mathbf{u} + \nabla p = \sum_{z \in \mathcal{Z}} \mathbf{F}_z \delta_z \text{ in } \Omega, \tag{78}$$

where  $\mathcal{Z} \subset \Omega$  denotes a finite set with cardinality  $\#\mathcal{Z}$  which is such that  $1 < \#\mathcal{Z} < \infty$  and  $\{\mathbf{F}_z\}_{z \in \mathcal{Z}} \subset \mathbb{R}^d$ . Based on the results of [4, Section 5], we introduce the weight

$$\rho(x) = \begin{cases} d_z^{\alpha}, & \exists z \in \mathcal{Z} : |x - z| < \frac{d_{\mathcal{Z}}}{2}, \\ 1, & |x - z| \ge \frac{d_{\mathcal{Z}}}{2}, \ \forall z \in \mathcal{Z}, \end{cases}$$

$$(79)$$

where  $d_{\mathcal{Z}} = \min \{ \text{dist}(\mathcal{Z}, \partial \Omega), \min \{ |z - z'| : z, z' \in \mathcal{Z}, z \neq z' \} \}$  and modify the definition (5), of the spaces  $\mathcal{X}$  and  $\mathcal{Y}$ , as follows:

$$\mathcal{X} = \mathbf{H}_0^1(\rho, \Omega) \times L^2(\rho, \Omega) / \mathbb{R}, \quad \mathcal{Y} = \mathbf{H}_0^1(\rho^{-1}, \Omega) \times L^2(\rho^{-1}, \Omega) / \mathbb{R}, \tag{80}$$

It can be proved that  $\rho$  belongs to the Muckenhoupt class  $A_2$  [41] and to the restricted class  $A_2(\Omega)$ .

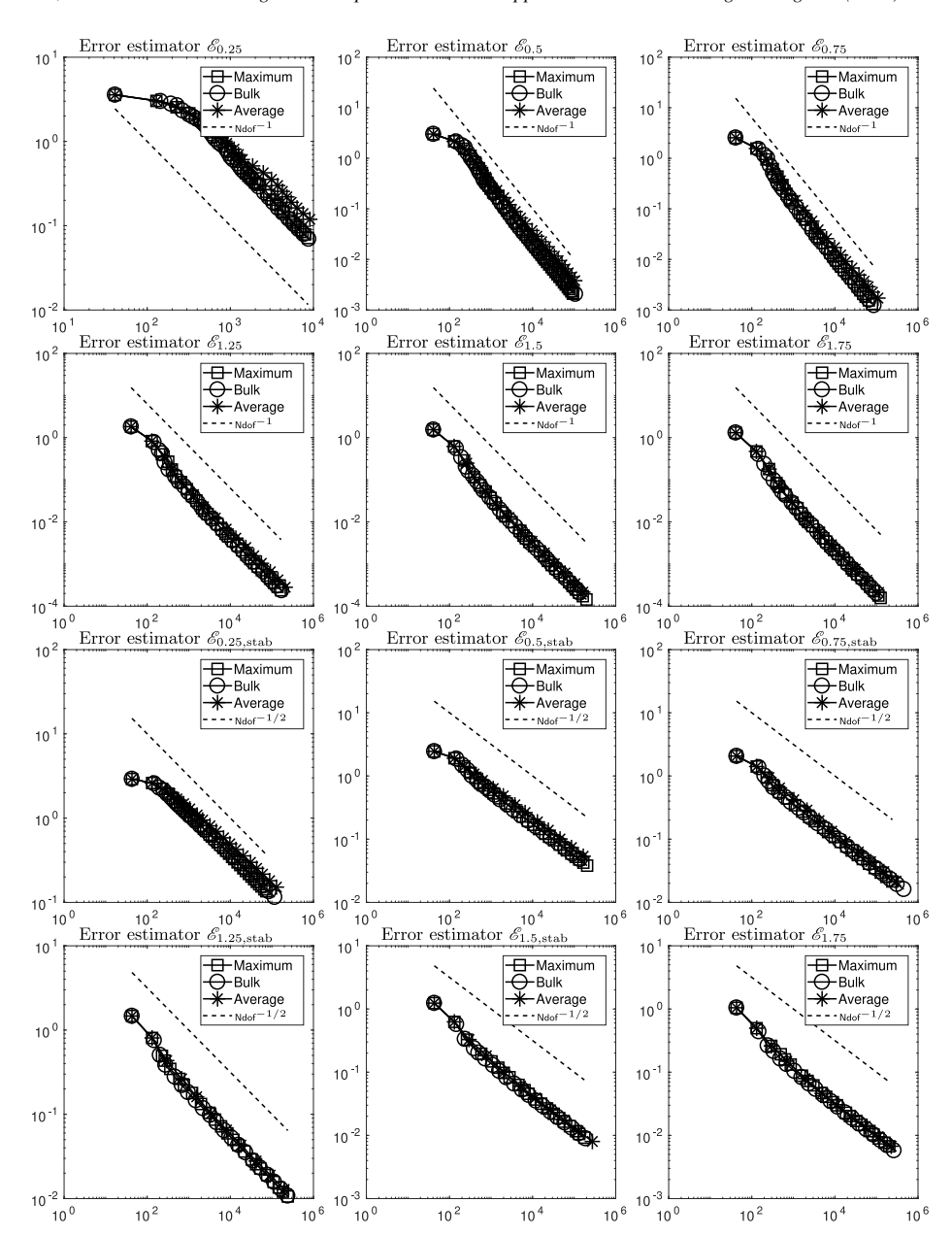


Fig. 3. Example 1: Experimental rates of convergence for the error estimators  $\mathcal{E}_{\alpha}$  and  $\mathcal{E}_{\alpha,stab}$  considering  $\alpha \in \{0.25, 0.5, 0.75, 1.25, 1.5, 1.75\}$  and three different marking strategies.

Define

$$D_{T,\mathcal{Z}} := \min_{z \in \mathcal{Z}} \left\{ \max_{x \in T} |x - z| \right\}. \tag{81}$$

We thus propose the following error estimator when the Taylor–Hood scheme is considered:

$$\mathscr{D}_{\alpha}(\mathbf{u}_{\mathscr{T}}, p_{\mathscr{T}}; \mathscr{T}) := \left(\sum_{T \in \mathscr{T}} \mathscr{D}_{\alpha}^{2}(\mathbf{u}_{\mathscr{T}}, p_{\mathscr{T}}; T)\right)^{\frac{1}{2}},$$

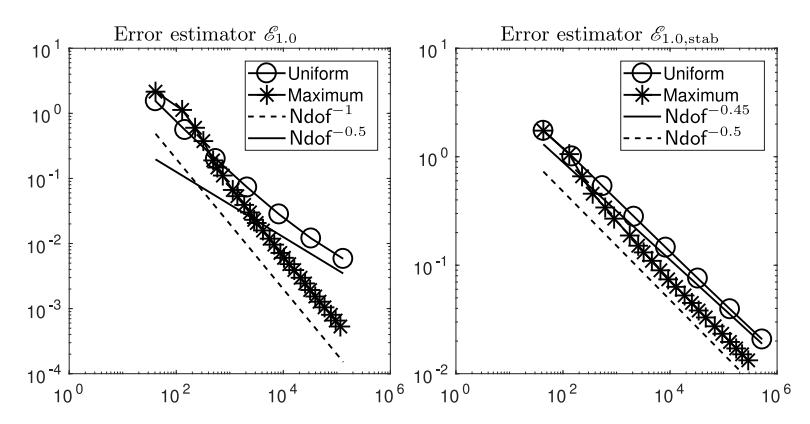


Fig. 4. Example 1: Experimental rates of convergence for the error estimators  $\mathcal{E}_{1.0}$  and  $\mathcal{E}_{1.0,stab}$  for uniform and adaptive refinement with the maximum strategy.

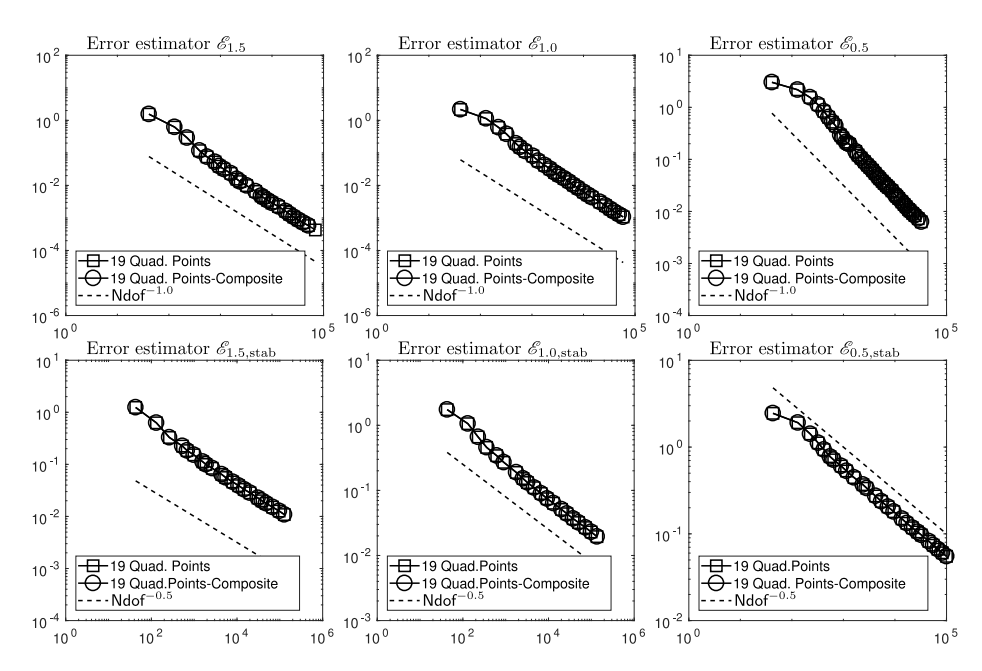


Fig. 5. Example 1: Experimental rates of convergence for the error estimators  $\mathscr{E}_{\alpha}$  and  $\mathscr{E}_{\alpha,\text{stab}}$  (maximum strategy), with  $\alpha \in \{0.5, 1.0, 1.5\}$ , based on a quadrature rule exact for polynomials of degree 19, and its composite counterpart. For mesh refinement, we have considered the maximum strategy.

where the local indicators are such that

$$\mathcal{D}_{\alpha}(\mathbf{u}_{\mathscr{T}}, p_{\mathscr{T}}; T) := \left( h_{T}^{2} D_{T, \mathscr{Z}}^{\alpha} \| \Delta \mathbf{u}_{\mathscr{T}} - \nabla p_{\mathscr{T}} \|_{\mathbf{L}^{2}(T)}^{2} + \| \operatorname{div} \mathbf{u}_{\mathscr{T}} \|_{L^{2}(\rho, T)}^{2} \right) + h_{T} D_{T, \mathscr{Z}}^{\alpha} \| \| (\nabla \mathbf{u}_{\mathscr{T}} - p_{\mathscr{T}} \mathbf{I}) \| \cdot \mathbf{v} \|_{\mathbf{L}^{2}(\partial T \setminus \partial \Omega)}^{2} + \sum_{z \in \mathscr{Z} \cap T} h_{T}^{\alpha + 2 - d} |\mathbf{F}_{z}|^{2} \right)^{\frac{1}{2}}.$$
(82)

Similarly, when the low-order stabilized approximation scheme is considered, we consider the error estimator

$$\mathcal{D}_{\alpha,\text{stab}}(\mathbf{u}_{\mathscr{T}}, p_{\mathscr{T}}; \mathscr{T}) := \left(\sum_{T \in \mathscr{T}} \mathcal{D}_{\alpha,\text{stab}}^2(\mathbf{u}_{\mathscr{T}}, p_{\mathscr{T}}; T)\right)^{\frac{1}{2}},$$

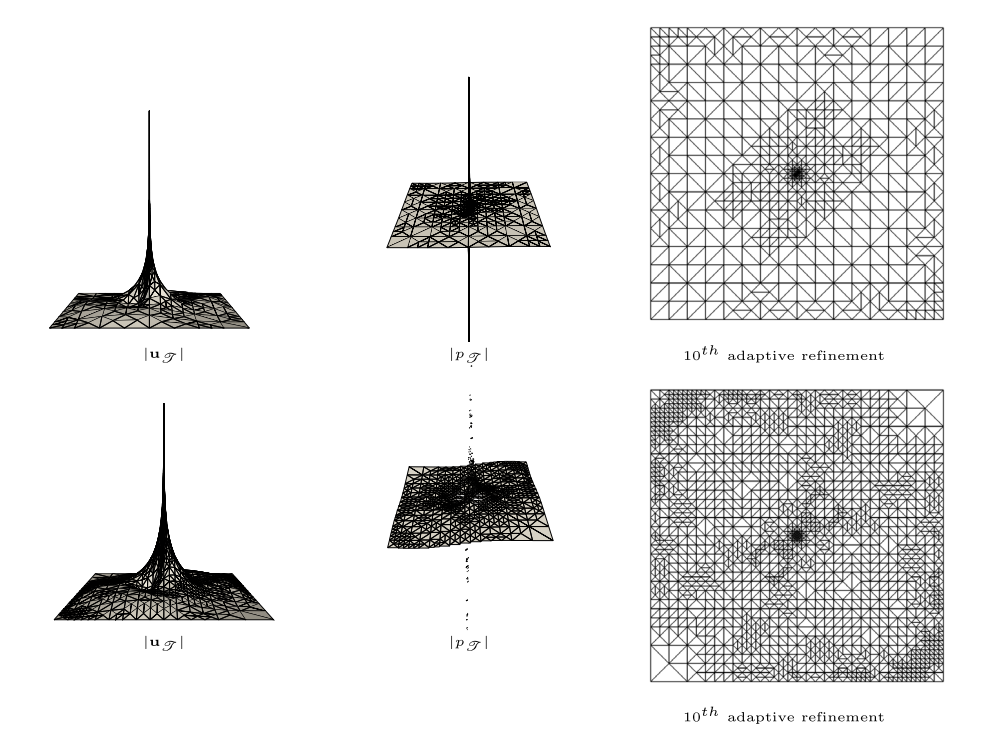


Fig. 6. Example 1: Finite element approximations of  $|\mathbf{u}_{\mathcal{T}}|$  and  $p_{\mathcal{T}}$  over the mesh obtained after 10 adaptive refinements, when a Taylor–Hood approximation is used with  $\mathcal{E}_{1.5}$  (maximum strategy (top)), and when the low-order stabilized approximation is considered with  $\mathcal{E}_{1.5,\text{stab}}$  (maximum strategy (bottom)).

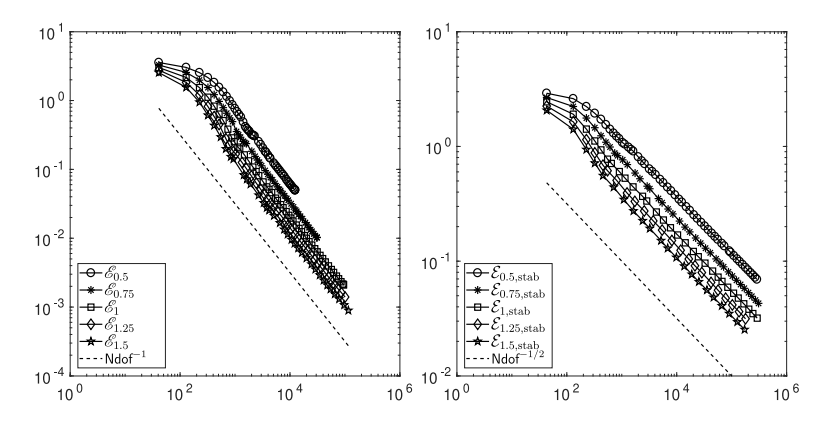


Fig. 7. Example 2: For  $\alpha = \{0.5, 0.75, 1, 1.25, 1.5\}$ , we present the experimental rates of convergence for the error estimators  $\mathcal{E}_{\alpha}$  (left) and  $\mathcal{E}_{\alpha,\text{stab}}$  (right), which are based on Taylor–Hood approximation and low-order stabilized approximation, respectively. For mesh refinement, we have considered the maximum strategy.

and the local error indicators

$$\begin{split} \mathcal{D}_{\alpha, \text{stab}}(\mathbf{u}_{\mathcal{T}}, p_{\mathcal{T}}; T) &:= \left( h_T^2 D_{T, \mathcal{Z}}^{\alpha} \| \Delta \mathbf{u}_{\mathcal{T}} - \nabla p_{\mathcal{T}} \|_{\mathbf{L}^2(T)}^2 + (1 + \tau_{\text{div}}^2) \| \operatorname{div} \mathbf{u}_{\mathcal{T}} \|_{L^2(\rho, T)}^2 \right. \\ &+ h_T D_{T, \mathcal{Z}}^{\alpha} \| \left[ \left[ (\nabla \mathbf{u}_{\mathcal{T}} - p_{\mathcal{T}} \mathbf{I}) \right] \cdot \mathbf{v} \|_{\mathbf{L}^2(\partial T \setminus \partial \Omega)}^2 + \sum_{z \in \mathcal{Z} \cap T} h_T^{\alpha + 2 - d} |\mathbf{F}_z|^2 \right)^{\frac{1}{2}}. \end{split}$$

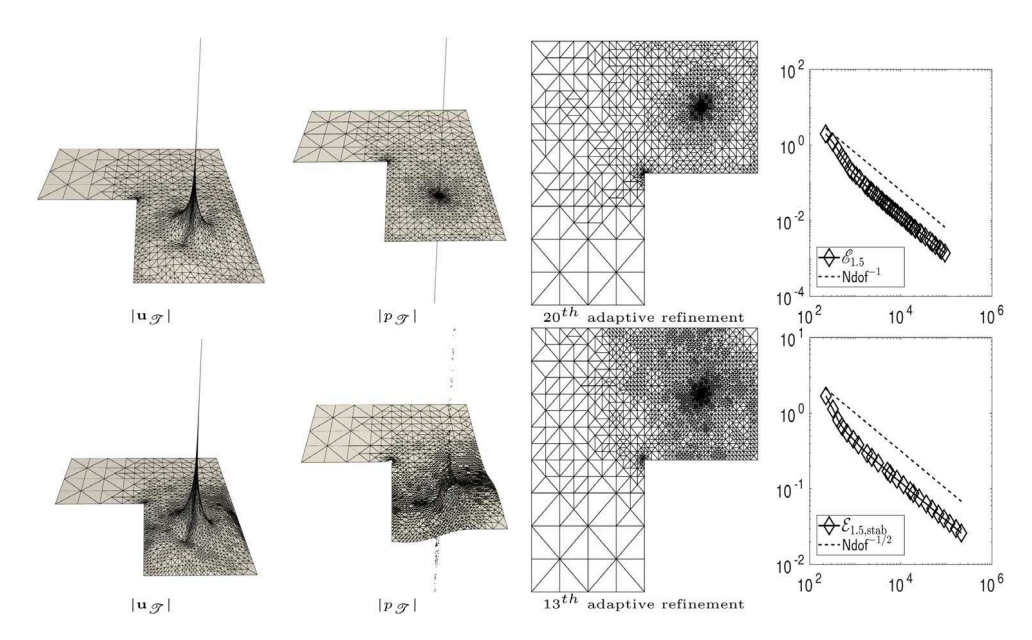


Fig. 8. Example 2: Finite element approximations of  $|\mathbf{u}_{\mathcal{T}}|$  and  $p_{\mathcal{T}}$ , the mesh obtained after M adaptive refinements, and the experimental rate of convergence for the error estimator when Taylor–Hood approximation is used (top) and when the low-order stabilized approximation is considered (bottom); M = 20 (top) and M = 13 (bottom). For mesh refinement, we have considered the maximum strategy.

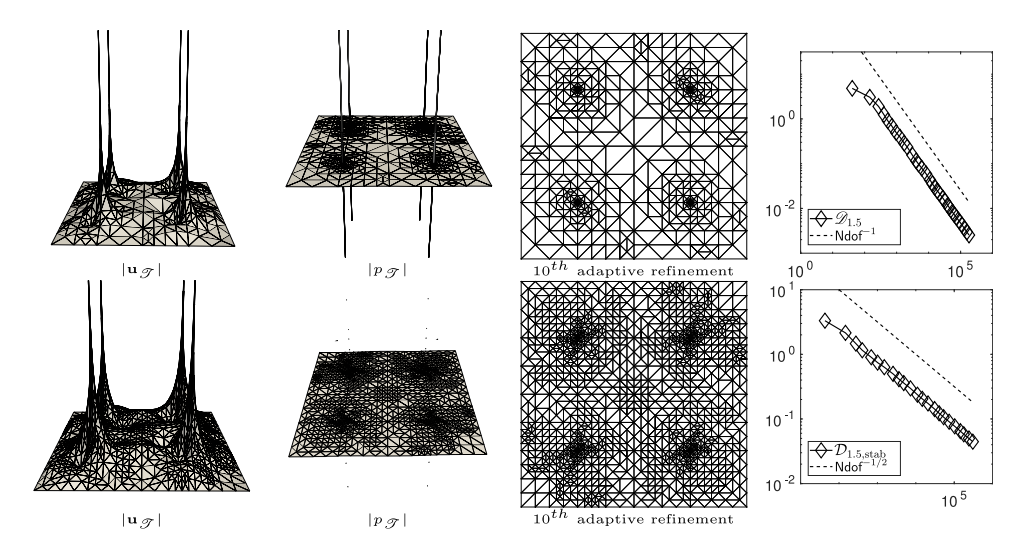


Fig. 9. Example 3: Finite element approximations of  $|\mathbf{u}_{\mathcal{T}}|$  and  $p_{\mathcal{T}}$ , the meshes obtained after 10 adaptive refinements, and the experimental rates of convergence when Taylor–Hood approximation is used (top) and when the low-order stabilized approximation is considered (bottom). For mesh refinement, we have considered the maximum strategy.

Having defined the problem and estimators we, in particular, set  $\Omega = (0, 1)^2$  and let

$$\mathcal{Z} = \{(0.25, 0.25)^{\mathsf{T}}, (0.25, 0.75)^{\mathsf{T}}, (0.75, 0.25)^{\mathsf{T}}, (0.75, 0.75)^{\mathsf{T}}\}.$$

We consider  $\mathbf{F}_z = (1, 1)^{\mathsf{T}}$  for all  $z \in \mathcal{Z}$  and fix the exponent of the Muckenhoupt weight  $\rho$ , which is defined in (79), as  $\alpha = 1.5$ .

In Fig. 9, we present the results obtained by the Algorithm 1 when is driven by  $\mathcal{D}_{1.5}$  (Taylor–Hood approximation) and  $\mathcal{D}_{1.5,\text{stab}}$  (low-order stabilized approximation) and the maximum strategy is considered. We present the finite element approximations of  $|\mathbf{u}_{\mathcal{T}}|$  and  $p_{\mathcal{T}}$  and the final meshes obtained by the aforementioned schemes. It can be

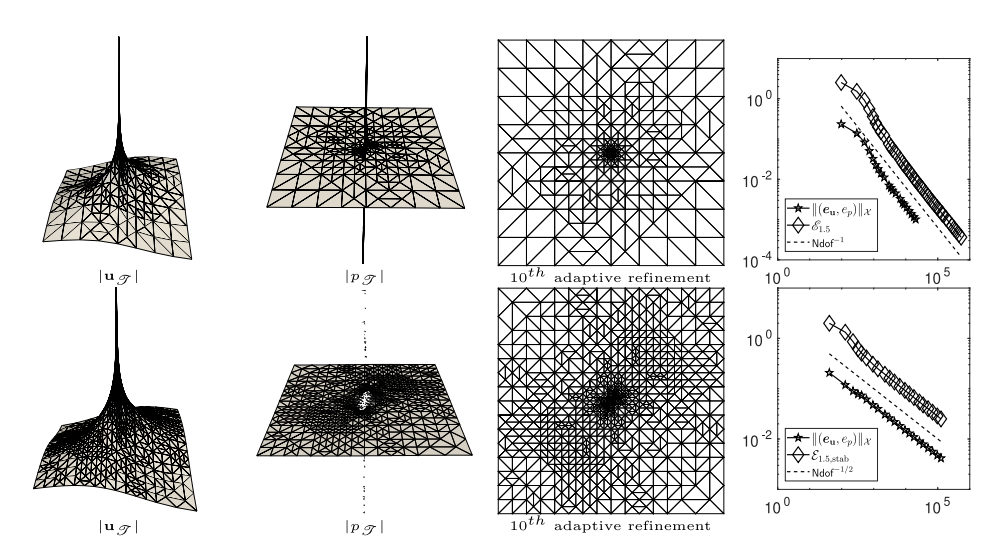


Fig. 10. Example 4: Finite element approximation of  $|\mathbf{u}_{\mathcal{T}}|$  and  $p_{\mathcal{T}}$ , the mesh obtained after 10 adaptive refinements, and the experimental rate of convergence for the error estimator when Taylor–Hood approximation is used (top) and when the low-order stabilized approximation is considered (bottom) where  $\alpha \in \{0.5, 0.75, 1, 1.25, 1.5\}$ . For mesh refinement, we have considered the maximum strategy.

observed that the proposed error estimators attained optimal experimental rates of convergence, under the natural proposed modification of the involved Muckenhoupt weight.

## 6.4. Example 4: The fundamental solution of a Stokes flow

In order to measure the experimental rates of convergence for the total error (74), we invoke the fundamental solution of the Stokes problem; even when we violate the assumption of imposing homogeneous boundary conditions. For a delta source  $\delta_z$ , located at  $z = (x_0, y_0)^T \in \Omega$ , and a given constant vector  $\mathbf{F} \in \mathbb{R}^2$ , we recall the fundamental solution for the Stokes problem (1) when d = 2:

$$\mathbf{u}(x,y) := \tilde{\mathbf{T}} \cdot \mathbf{F}, \quad p(x,y) := \mathbf{T} \cdot \mathbf{F}, \tag{83}$$

where, if  $\mathbf{x}_0 = (x - x_0, y - y_0)^{\mathsf{T}}$ , then

$$\begin{split} \tilde{\mathbf{T}} &= -\frac{1}{4\pi} \left( \log |\mathbf{x}_0| \begin{bmatrix} 1 & 0 \\ 0 & 1 \end{bmatrix} - \frac{1}{|\mathbf{x}_0|^2} \begin{bmatrix} (x - x_0)^2 & (x - x_0)(y - y_0) \\ (x - x_0)(y - y_0) & (y - y_0)^2 \end{bmatrix} \right), \\ \mathbf{T} &= \frac{\mathbf{x}_0}{2\pi |\mathbf{x}_0|^2}. \end{split}$$

We consider  $\Omega = (0, 1)^2$ ,  $z = (0.5, 0.5)^{\mathsf{T}}$  and  $\mathbf{F} = (1, 1)^{\mathsf{T}}$  in problem (1). We fix the exponent of the Muckenhoupt weight in (3) as  $\alpha = 1.5$ . The solution of this problem is thus given by (83).

In Fig. 10, we present the finite element approximations of  $|\mathbf{u}_{\mathcal{T}}|$  and  $p_{\mathcal{T}}$  which were obtained after 10 adaptive refinements (maximum strategy), together with the final mesh. We also present the experimental rates of convergence for the total error  $\|(\mathbf{e}_{\mathbf{u}}, e_p)\|_{\mathcal{X}}$  and the error estimators  $\mathcal{E}_{1.5}$  and  $\mathcal{E}_{\alpha,\text{stab}}$ . It can be observed that optimal experimental rates of convergence are attained and that most of the adaptive refinement is concentrated around the delta source. In Fig. 11, we present the experimental rate of convergence for the total error estimators  $\mathcal{E}_{\alpha}$  and  $\mathcal{E}_{\alpha,\text{stab}}$  when  $\alpha \in \{0.5, 0.75, 1, 1.25, 1.5\}$ . It can be observed that, for all the cases that we have considered, optimal rates of convergence are attained.

Finally, in Fig. 12 we present the finite element approximations  $|\mathbf{u}_{\mathcal{T}}|$  and  $p_{\mathcal{T}}$  which were obtained after 15 adaptive refinements when using the residual-type error indicators  $\mathcal{E}_{rg,1}(\mathbf{u}_{\mathcal{T}}, p_{\mathcal{T}}; T)$  to drive the adaptive procedure, by fixing the constant  $a = 10^{-6}$  (maximum strategy). We also present the experimental rates of convergence for the velocity error  $\|\mathbf{u} - \mathbf{u}_{\mathcal{T}}\|_{\mathbf{L}^2(\Omega)}$  and the error estimator  $\mathcal{E}_{rg,1}$ . It can be observed that even when the adaptive refinement is concentrated around the delta source, the velocity error does not converge at all and that the residual-type a posteriori

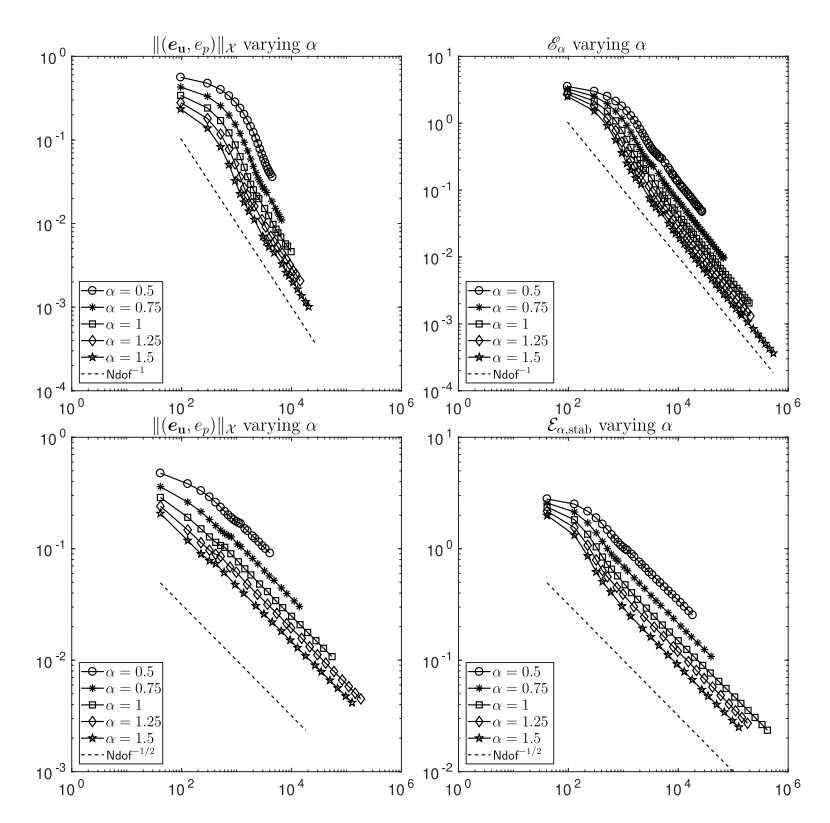


Fig. 11. Example 4: Experimental rates of convergence for the total error  $\|(e_{\mathbf{u}}, e_p)\|_{\mathcal{X}}$  and error estimators  $\mathscr{E}_{\alpha}$  (Taylor–Hood approximation) and  $\mathcal{E}_{\alpha,\text{stab}}$  (low-order stabilized approximation).

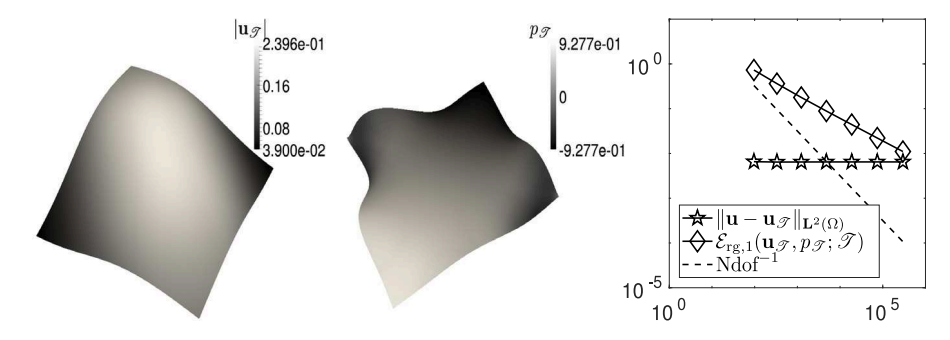


Fig. 12. Example 4: Finite element approximation of  $|\mathbf{u}_{\mathcal{T}}|$  and  $p_{\mathcal{T}}$  over a mesh obtained after 4 adaptive refinements, and the experimental rate of convergence for the residual-type error estimator  $\mathcal{E}_{rg,1}(\mathbf{u}_{\mathcal{T}},p_{\mathcal{T}};\mathcal{T})$  when a Taylor–Hood approximation is used and the adaptive procedure is driven by the residual-type error indicators  $\mathcal{E}_{rg,1}(\mathbf{u}_{\mathcal{T}},p_{\mathcal{T}};K)$  where  $a=10^{-6}$ . For mesh refinement, we have considered the maximum strategy.

error estimator does not present optimal convergence rate. This should come as no surprise, as we are trying to measure the error in spaces that do not contain the exact solution. This further supplements the claim we made in Section 6.1: the rates of convergence that we observed there are just a preasymptotic phenomenon.

## References

- [1] A. Ern, J.-L. Guermond, Theory and Practice of Finite Elements, in: Applied Mathematical Sciences, vol. 159, Springer-Verlag, New York, 2004, p. xiv+524.
- [2] V. Girault, P.-A. Raviart, Finite Element Methods for Navier-Stokes Equations, in: Springer Series in Computational Mathematics, vol. 5, Springer-Verlag, Berlin, 1986, p. x+374, http://dx.doi.org/10.1007/978-3-642-61623-5, Theory and algorithms.

- [3] L. Lacouture, A numerical method to solve the Stokes problem with a punctual force in source term, C. R. Mec. 343 (3) (2015) 187–191, htt p://dx.doi.org/10.1016/j.crme.2014.09.008.
- [4] A. Allendes, E. Otárola, R. Rankin, A.J. Salgado, Adaptive finite element methods for an optimal control problem involving Dirac measures, Numer. Math. 137 (1) (2017) 159–197, http://dx.doi.org/10.1007/s00211-017-0867-9.
- [5] C. Brett, A. Dedner, C. Elliott, Optimal control of elliptic PDEs at points, IMA J. Numer. Anal. 36 (3) (2016) 1015–1050, http://dx.doi.org/10.1093/imanum/drv040.
- [6] L. Chang, W. Gong, N. Yan, Numerical analysis for the approximation of optimal control problems with pointwise observations, Math. Methods Appl. Sci. 38 (18) (2015) 4502–4520, http://dx.doi.org/10.1002/mma.2861.
- [7] M. Bulíček, J. Burczak, S. Schwarzacher, A unified theory for some non-Newtonian fluids under singular forcing, SIAM J. Math. Anal. 48 (6) (2016) 4241–4267, http://dx.doi.org/10.1137/16M1073881.
- [8] J. Duoandikoetxea, Fourier Analysis, in: Graduate Studies in Mathematics, vol. 29, American Mathematical Society, Providence, RI, 2001, p. xviii+222, Translated and revised from the 1995 Spanish original by David Cruz-Uribe.
- [9] V. Gol'dshtein, A. Ukhlov, Weighted Sobolev spaces and embedding theorems, Trans. Amer. Math. Soc. 361 (7) (2009) 3829–3850, http://d x.doi.org/10.1090/S0002-9947-09-04615-7.
- [10] R.H. Nochetto, E. Otárola, A.J. Salgado, Piecewise polynomial interpolation in Muckenhoupt weighted Sobolev spaces and applications, Numer. Math. 132 (1) (2016) 85–130, http://dx.doi.org/10.1007/s00211-015-0709-6.
- [11] B.O. Turesson, Nonlinear Potential Theory and Weighted Sobolev Spaces, in: Lecture Notes in Mathematics, vol. 1736, Springer-Verlag, Berlin, 2000, p. xiv+173, http://dx.doi.org/10.1007/BFb0103908.
- [12] R.G. Durán, A.L. Lombardi, Error estimates on anisotropic  $Q_1$  elements for functions in weighted Sobolev spaces, Math. Comp. 74 (252) (2005) 1679–1706, http://dx.doi.org/10.1090/S0025-5718-05-01732-1.
- [13] J.P. Agnelli, E.M. Garau, P. Morin, *A posteriori* error estimates for elliptic problems with Dirac measure terms in weighted spaces, ESAIM Math. Model. Numer. Anal. 48 (6) (2014) 1557–1581, http://dx.doi.org/10.1051/m2an/2014010.
- [14] B. Muckenhoupt, Weighted norm inequalities for the Hardy maximal function, Trans. Amer. Math. Soc. 165 (1972) 207–226, http://dx.doi.org/10.2307/1995882.
- [15] R. Farwig, H. Sohr, Weighted L<sup>q</sup>-theory for the Stokes resolvent in exterior domains, J. Math. Soc. Japan 49 (2) (1997) 251–288, http://dx.doi.org/10.2969/jmsj/04920251.
- [16] E. Otárola, A.J. Salgado, The Poisson and Stokes problems on weighted spaces in Lipschitz domains and under singular forcing, J. Math. Anal. Appl. 471 (1–2) (2019) 599–612, http://dx.doi.org/10.1016/j.jmaa.2018.10.094.
- [17] E.B. Fabes, C.E. Kenig, R.P. Serapioni, The local regularity of solutions of degenerate elliptic equations, Comm. Partial Differential Equations 7 (1) (1982) 77–116, http://dx.doi.org/10.1080/03605308208820218.
- [18] G.P. Galdi, An Introduction to the Mathematical Theory of the Navier-Stokes Equations, second ed., in: Springer Monographs in Mathematics, Springer, New York, 2011, p. xiv+1018, http://dx.doi.org/10.1007/978-0-387-09620-9, Steady-state problems.
- [19] V. Kozlov, V. Maz'ya, J. Rossmann, Elliptic Boundary Value Problems in Domains with Point Singularities, American Mathematical Society, Providence, Rhode Island, USA, 1997.
- [20] J.R. Nečas, Les Méthodes Directes en Théorie des Équations Elliptiques, Academia, Éditeurs, Prague, Masson et Cie, Éditeurs, Paris, 1967, p. 351.
- [21] J. Nečas, Sur une méthode pour résoudre les équations aux dérivées partielles du type elliptique, voisine de la variationnelle, Ann. Scuola Norm. Sup. Pisa (3) 16 (1962) 305–326.
- [22] R.H. Nochetto, K.G. Siebert, A. Veeser, Theory of adaptive finite element methods: an introduction, in: Multiscale, Nonlinear and Adaptive Approximation, Springer, 2009, http://dx.doi.org/10.1007/978-3-642-03413-8\_12.
- [23] P.G. Ciarlet, The Finite Element Method for Elliptic Problems, SIAM, Philadelphia, PA, 2002, p. xxviii+530, http://dx.doi.org/10.1137/1.97 80898719208.
- [24] D.N. Arnold, F. Brezzi, M. Fortin, A stable finite element for the Stokes equations, Calcolo 21 (4) (1984) 337–344 (1985), http://dx.doi.org/10.1007/BF02576171.
- [25] P. Hood, C. Taylor, Navier-Stokes equations using mixed interpolation, Finite Elem. Methods Flow Prob. (1974) 121–132.
- [26] R. Verfürth, A posteriori error estimators for the Stokes equations, Numer. Math. 55 (3) (1989) 309–325, http://dx.doi.org/10.1007/BF01390 056.
- [27] R. Verfürth, A Posteriori Error Estimation Techniques for Finite Element Methods, in: Numerical Mathematics and Scientific Computation, Oxford University Press, Oxford, 2013, p. xx+393, http://dx.doi.org/10.1093/acprof:oso/9780199679423.001.0001.
- [28] P. Clément, Approximation by finite element functions using local regularization, Rev. Fr. Automat. Inf. Rech. Opér. Sér. 9 (R-2) (1975) 77–84.
- [29] L.R. Scott, S. Zhang, Finite element interpolation of nonsmooth functions satisfying boundary conditions, Math. Comp. 54 (190) (1990) 483–493, http://dx.doi.org/10.2307/2008497.
- [30] T.J.R. Hughes, L.P. Franca, M. Balestra, A new finite element formulation for computational fluid dynamics. V. Circumventing the Babuška-Brezzi condition: a stable Petrov-Galerkin formulation of the Stokes problem accommodating equal-order interpolations, Comput. Methods Appl. Mech. Engrg. 59 (1) (1986) 85–99, http://dx.doi.org/10.1016/0045-7825(86)90025-3.
- [31] H.-G. Roos, M. Stynes, L. Tobiska, Robust Numerical Methods for Singularly Perturbed Differential Equations, second ed., in: Springer Series in Computational Mathematics, vol. 24, Springer-Verlag, Berlin, 2008, p. xiv+604, Convection-diffusion-reaction and flow problems.
- [32] P.B. Bochev, M.D. Gunzburger, Least-Squares Finite Element Methods, in: Applied Mathematical Sciences, vol. 166, Springer, New York, 2009, p. xxii+660, http://dx.doi.org/10.1007/b13382.
- [33] V. John, Finite Element Methods for Incompressible Flow Problems, in: Springer Series in Computational Mathematics, vol. 51, Springer, Cham, 2016, p. xiii+812, http://dx.doi.org/10.1007/978-3-319-45750-5.

- [34] D. Kay, D. Silvester, A posteriori error estimation for stabilized mixed approximations of the Stokes equations, SIAM J. Sci. Comput. 21 (4) (1999/00) 1321–1336.
- [35] P.R. Amestoy, I.S. Duff, J.-Y. L'Excellent, J. Koster, A fully asynchronous multifrontal solver using distributed dynamic scheduling, SIAM J. Matrix Anal. Appl. 23 (1) (2001) 15–41, http://dx.doi.org/10.1137/S0895479899358194 (electronic).
- [36] P.R. Amestoy, A. Guermouche, J.-Y. L'Excellent, S. Pralet, Hybrid scheduling for the parallel solution of linear systems, Parallel Comput. 32 (2) (2006) 136–156, http://dx.doi.org/10.1016/j.parco.2005.07.004.
- [37] W. Dörfler, A convergent adaptive algorithm for Poissons equation, SIAM J. Numer. Anal. 33 (3) (1996) 1106–1124.
- [38] X. Deng, Y. Zhao, J. Zou, On linear finite elements for simultaneously recovering source location and intensity, Int. J. Numer. Anal. Model. 10 (3) (2013).
- [39] B. Hosseini, N. Nigam, J.M. Stockie, On regularizations of the Dirac delta distribution, J. Comput. Phys. 305 (2016) 423–447, http://dx.doi. org/10.1016/j.jcp.2015.10.054.
- [40] R. Verfürth, A posteriori error estimators for the Stokes equations, Numer. Math. 55 (3) (1989) 309–325.
- [41] H. Aimar, M. Carena, R. Durán, M. Toschi, Powers of distances to lower dimensional sets as Muckenhoupt weights, Acta Math. Hungar. 143 (1) (2014) 119–137, http://dx.doi.org/10.1007/s10474-014-0389-1.